REDUCTION IN INTER-SYMBOL INTERFERENCE USING LINEAR PROLATE FUNCTIONS

by

Sagar Sushil Soman

Submitted in partial fulfilment of the requirements

for the degree of Master of Applied Science

at

Dalhousie University

Halifax, Nova Scotia

March 2015

TABLE OF CONTENTS

List of Figures

Abstract

In a baseband system, the digital information signal required to be transmitted over a channel, has a wide frequency spectrum. This wide frequency spectrum gets attenuated due to the band limited response of the filters utilized for communication. This band limiting of the signal pulses, causes them to expand outward thereby interfering with each other and causing a phenomenon known as Inter-Symbol Interference. The known techniques used for avoiding this limitation have used bandwidth greater than the minimum required bandwidth for no interference given by Nyquist. The physical increase in bandwidth of the filters can cause high frequency noise to interfere with the transmitted information signal. This thesis presents an innovative way to reduce Inter-Symbol Interference in the received signal by utilising a special filter designed by using Linear Prolate Functions. The results compare the signal reconstruction capabilities of a prolate filter with those of an ideal low pass filter.

List Of Abbreviations And Symbols Used

dc	Direct current
KHz	Kilo Hertz
MHz	Mega Hertz
NRZ	Non Return to zero
a_k	Unipolar non return to zero signal
I_K	Data bits generated at the transmitter
$g(t)$	Impulse response of the transmit filter
$s(t)$	Output of the transmit filter
$H(f)$	Frequency response of the channel
$c(t)$	Impulse response of the receive filter
$\mu p(t)$	Scaled pulse obtained by convolving the impulse response of the transmit filter, channel and the receive filter
$h(t)$	Impulse response of the channel
$G(f)$	Frequency response of the transmit filter
$C(f)$	Frequency response of the receive filter
∞	Infinity
W	Absolute bandwidth of the filter
W_0	Minimum Nyquist bandwidth for rectangular low pass filter and -6db bandwidth for raised cosine filter
db	decibels
r	Roll-off factor

M	Threshold Value of the prolate filter
$r^2(t)\ and\ \lvert R(f)\rvert^2$	Probability density of a signal $r(t)$ with unit energy
$\sigma_r\ and\ \sigma_R$	Variances of the signal $r(t)$
$\alpha^2(T)$	Measure of concentration of the signal $r(t)$
k	Wave vector
λ	Wavelength
c	Space-bandwidth product parameter
S	Angular component of Helmholtz wave equation in spheroidal co-ordinate system
R	Radial component of Helmholtz wave equation in spheroidal co-ordinate system
ψ_n	Linear Prolate Function of order 'n'
λ_n	Eigenvalue of the Linear Prolate Function
t_0	Time-limited interval which has a range of $[-1, +1]$
Ω_0	Finite bandwidth to be considered which has a range of $[-c, +c]$
$n_{critical}$	Critical Value of the order 'n'
$n\ \sin\theta$	Numerical Aperture of an imaging system
d	Minimum limit at which the imaging system is just able to separate two point responses as separate entities
λ_0	Wavelength of light in vacuum
$A_0, A_1, \ldots$	Complex amplitudes of the signal radiated by an end fire array antenna
l	Spacing between elements of an end fire array antenna

$G(f_x, f_y)$	Frequency spectrum of a signal
G_{mn}	Fourier coefficients of a signal
$b(\xi)$	Complex amplitude of an image
$a(x)$	Complex amplitude of an object
$g(\xi, x)$	Imaging kernel or amplitude response obtained from the imaging system
$\delta(x)$	Dirac delta function in the time domain
$U_M(\omega)$	Pupil Function of the prolate filter with threshold value 'M'
BW	Bandwidth
IC	Integrated circuit

Acknowledgements

I would like to thank my supervisor Dr. Michael Cada for giving me an opportunity to work on this research topic. His continuous guidance and support has helped me throughout my graduate school experience. His advice of relating problems of different areas in electrical engineering with each other has made understanding and solving them much easier for me. His constructive evaluations during group meetings has helped me improve my problem solving and presentation skills.

I additionally would like to express my gratitude towards the entire photonics lab group for their continuous support and assistance with my thesis work. Moreover, I want to thank Dr. Jason Gu and Dr. William Phillips for being a part of my thesis committee.

I also want to thank my family as all of my accomplishments would not have been possible without their sacrifice and unending emotional support. Furthermore, I want to thank my friends and roommates for making my stay in Canada a pleasant and enjoyable one.

CHAPTER 1: INTRODUCTION

The term 'Baseband Transmission' refers to the transmission of low frequency digital data i.e. a signal whose frequency range extends from zero or dc (direct current) value to a certain finite value [1]. In telephony the baseband signal bandwidth extends from 0 to 3.5 KHz. In television the baseband is the video band occupying 0 to 4.3 MHz. Similarly, for digital data using unipolar signalling at the rate of F_b pulses per second, the baseband signal bandwidth extends from 0 to F_b Hz [2]. Baseband transmission is performed without any modulation because the baseband pulses have sizeable power such that they can be transmitted satisfactorily through different channels. Common examples of baseband channels are optical fibers, twisted pair cables and co-axial cables. Digital data in its raw form is not compatible with the different baseband channels mentioned before. Hence before transmission, this data is converted into rectangular pulses which are compatible with every basebands channel used in today's applications [3].

Digital data has a wide frequency spectrum and in order to transmit such a broad spectrum of data, the channel must ideally contain a flat pass band and a bandwidth large enough to pass all the frequencies [1]. In reality, most channels have a response which causes the digital pulses to expand thereby affecting adjoining pulses leading to a phenomenon known as Inter-Symbol Interference (ISI). Inter-Symbol Interference is caused in transmission by two main factors namely:

- Band-limited frequency response of the filter at the receiver
- Additive white Gaussian noise present in the channel.

The major focus of this thesis will be to reduce Inter-Symbol Interference caused by band-limited frequency response of the filter at the receiver. The inter-symbol interference impedes the correct formation of the signal at the receiver which causes bit errors in the reconstructed data stream. In order to eliminate this effect different pulse shaping techniques are used such as:

- Reducing the width of the impulse response of the transmitted signal so that eventually when the impulses do expand after passing through the channel they will not affect each other.
- Creating raised cosine impulses which causes the sidebands to have a reduced amplitude thereby reducing the interference between sidebands of the previously transmitted symbol and main lobe of the next symbol.
- Using a guard time period between two impulses so that the impulses are given enough room to expand which minimizes the probability of interference between them.

In baseband transmission, the main objective is to reduce the required system bandwidth as much as possible. For instance, in case of a telephone channel the amount of bandwidth available to each user is much less because different users utilize the same channel at the same time. Hence, by keeping the bandwidth available for each user to a minimum, the data rate can be increased and in turn lead to a greater utilization of total available bandwidth in the channel [3]. The last two pulse shaping techniques mentioned previously require additional bandwidth as compared to the bandwidth required by the first technique.

In this thesis, an innovative approach will be shown which will perform significantly better than other two techniques mentioned before. This approach will lead to a highly precise signal reconstruction at the receiver, while satisfying the main objective of a baseband communication system. This approach was possible because of Linear Prolate Functions. These functions have some favourable properties which can be utilised to resolve some of the shortcomings in various applications in optics and signal processing. The only reason these functions have not been researched thoroughly in the signal processing field and its various applications is because it is too complicated to calculate them accurately. This major limitation has been overcome in this research by utilizing a proprietary algorithm which calculates highly accurate Linear Prolate functions in a software known as Mathematica.

1.1. Motivation

Baseband transmission is a branch of Electrical engineering in which digital data in the form of rectangular pulses with lower frequencies and sizeable power is transmitted from a transmitter to a receiver via a baseband channel. These pulses undergo distortions as they travel through the channel and this phenomenon is known as inter-symbol interference. A filter is generally employed at the receiver to reduce this interference. But due to the band limited nature of the filter response, the signal is not reproduced accurately at the receiver.

Nyquist [4] had proposed a criteria for the filter bandwidth by which transmission of the digital data can be done without any interference. However, this criteria when implemented practically also had its flaws which will be discussed later. The other methods which modify the filter response to reduce this interference require additional bandwidth as compared to the bandwidth required by the method proposed by Nyquist. Hence, there is a need for a technique which can provide interference reducing capability with less bandwidth consumption. This research hopes to fulfill that need by studying and simulating a filter which was designed using linear prolate functions. The prolate functions greatly enhances the inter-symbol interference reducing capability of the filter and the total bandwidth consumed to achieve this is equal to the Nyquist bandwidth. In this thesis, most of the illustration explained through graphs have their axes normalized and hence will have no specific units mentioned for them. Furthermore, the application of linear prolate function in the field of digital communication will be the main original contribution of this research.

1.2. Sampling and Aliasing

Before introducing Inter-symbol Interference and studying its effects at the receiver of a baseband communication system, one needs to understand aliasing which is an effect occurring at the transmitter of a communication system. Aliasing primarily occurs while converting an analog signal into a digital signal. The first step of any analog to digital converter is sampling. If the analog signal is sampled at a lower sampling rate, aliasing occurs in the system. In order to comprehend aliasing and its effects the sampling theorem put forth by Nyquist has to be understood.

The sampling theorem states that a band-limited signal can be reconstructed exactly from its samples, if the sampling frequency is greater than twice the maximum frequency of the signal being sampled [2]. The sampling theorem can be can be analysed as follows [2]:

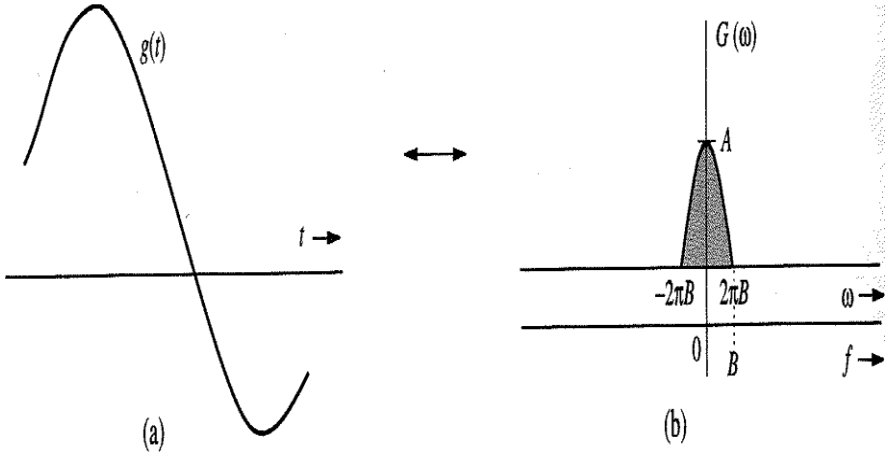

Figure 1.1. A Signal and its Frequency Spectrum [2]

Consider an analog signal $g(t)$ whose frequency spectrum is band-limited to B Hz as shown in Figure 1.1. The signal is sampled with the help of a discrete train of impulses

with a rate of f_s Hz. The sampled signal is thus obtained by multiplication of the signal $g(t)$ with the train of impulses δT_s where $T_s = \frac{1}{f_s}$. Hence,

$$\bar{g}(t) = g(t)\delta T_s = \sum_n g(nT_s)\delta(t - nT_s) \tag{1.1}$$

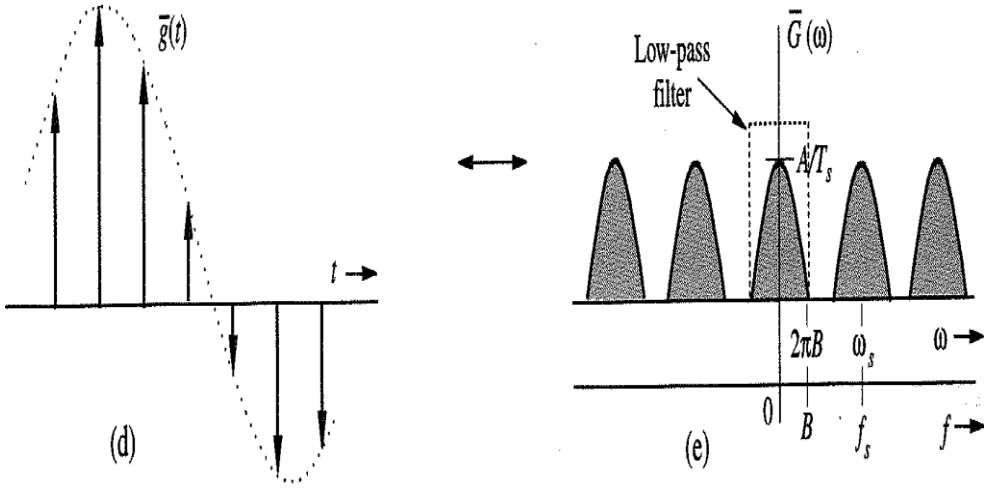

Figure 1.2. A Sampled Signal and its corresponding Frequency Spectrum [2]

Any periodic signal can be represented by a Fourier series and as the impulses are periodic in nature, they can also be represented by a Fourier series as follows:

$$\delta T_s(t) = \frac{1}{T_s}[1 + 2\cos(\omega_s t) + 2\cos(2\omega_s t) + 2\cos(3\omega_s t) + \cdots] \tag{1.2}$$

Thus, $\bar{g}(t)$ can be represented as follows:

$$\bar{g}(t) = \frac{1}{T_s}[g(t) + 2g(t)\cos(\omega_s t) + 2g(t)\cos(2\omega_s t) + 2g(t)\cos(3\omega_s t) + \cdots] \tag{1.3}$$

In order to obtain the frequency spectrum of the sampled signal, Fourier transform operation has to be performed on Equation (1.3). Hence, the Fourier transform of the first

term in Equation (1.3) is $G(\omega)$. The Fourier transform of the second term is $G(\omega - \omega_s) + G(\omega + \omega_s)$. This means that the spectrum $G(\omega)$ has shifted to $-\omega_s$ and $+\omega_s$ as shown in Figure 1.2. The samples of $G(\omega)$ will continue to be shifted to $-n\omega_s$ and $+n\omega_s$ until it reaches infinity. This shows that the spectrum of the sampled signal consists of periodically repeating samples of the spectrum $G(\omega)$.

$$\bar{G}(\omega) = \frac{1}{T_s} \sum_{n=-\infty}^{\infty} G(\omega - \omega_s) \tag{1.4}$$

In order to reconstruct the original signal the fundamental frequency $G(\omega)$ is required. This can be done by utilizing an ideal low pass filter with a frequency response which is same as the maximum bandwidth B as shown in Figure 1.2. The sampling frequency should not be considered equal to twice the maximum bandwidth. This is because in practise, it is difficult to fabricate an ideal low pass filter and the practical filters generally have a transition band where the filter transitions from pass band to stop band. Thus for exact reconstruction of the analog signal from its samples the sampling frequency must be greater than twice the maximum bandwidth of the signal being sampled i.e.

$$f_s > 2B \tag{1.5}$$

Equation (1.5) is the analytical form of the sampling theorem as proposed by Nyquist. If the sampling rate is less than twice the maximum bandwidth then it leads to a phenomenon known as aliasing as shown in Figure 1.3:

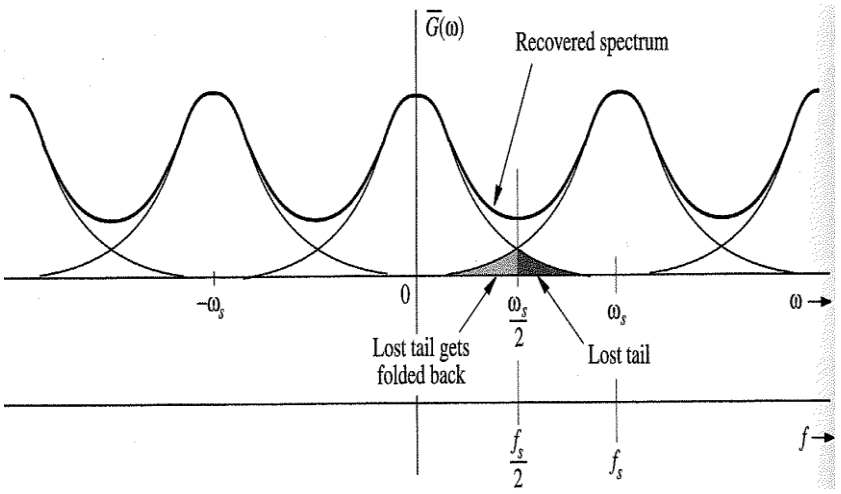

Figure 1.3. The Aliasing effect [2]

The sampling theorem was based on the assumption that the signal is band-limited. In reality, most signals are limited in the time-domain because of which they have a frequency spectrum which ideally spans up to infinity. As the signal cannot be time and band-limited at the same time, the overlapping of the frequency spectrum is a constant occurrence in any communication transmitter system. The aliasing effect can be avoided if a filtering process is used. This filter is termed as an anti-aliasing filter and it is present in many applications in use today. There are two ways in which anti-aliasing can be done namely pre-filtering and post-filtering [3]. In the pre-filtering process, the frequency spectrum of the analog signal is limited to a certain frequency namely $f_s/2$ before sampling due to which when the data is sampled there is no overlap between two spectral components. On the other hand, for a post filtering process the filtering operation is done after the sampling process. After the aliasing has occurred the filter attenuates the frequencies beyond $f_s/2$. In both cases there is appreciable loss of signal components.

1.3. Inter-Symbol Interference

There are many different kinds of noise present in a system but this thesis will primarily focus on Inter-Symbol Interference and provide a solution to reduce its effects. Inter-Symbol Interference is a kind of signal distortion in which the transmitted pulses expand outward after being transmitted through a channel and filtered through filters. Due to this expansion they interfere with each other as shown in the Figure 1.4:

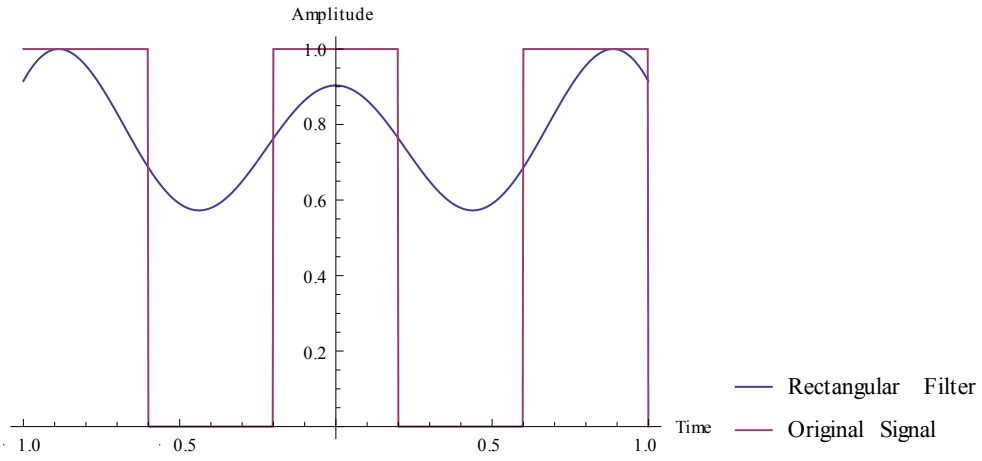

Figure 1.4. Inter-Symbol Interference in a Signal

The following derivation as in [1] helps in understanding inter-symbol interference analytically. Consider a digital communication system as seen in Figure 1.5:

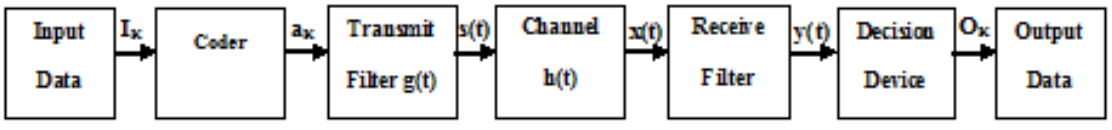

Figure 1.5. A Digital Communication System

In this system, the binary information signal is encoded by a line coder. Essentially a line coder is similar to a pulse amplitude modulator where in it assigns a certain amplitude to a

certain bit. The coder converts the information signal into a unipolar non-return to zero (NRZ) signal i.e.

$$a_k = \begin{cases} 1 \; if \; I_K = 1 \\ 0 \; if \; I_K = 0 \end{cases} \tag{1.6}$$

A Coder is utilized in this case as it is more suitable to transmit pulse waveforms instead of individual data bits through the channel. The sequence of short pulses are then passed through a transmit filter having an impulse response $g(t)$.

$$s(t) = \sum_k a_k * g(t - KT_b) \tag{1.7}$$

The transmit filter shown in a baseband transmission system is used as an anti-aliasing filter. This signal is then passed through a channel which has a band-limited frequency response $H(f)$ where $H(f) = 0$ for frequencies above a cut-off frequency. Since the major focus of this thesis is to reduce inter-symbol interference caused by band limited nature of the devices, the additive white Gaussian noise is assumed to be zero. This noisy signal is then passed through the receive filter with response $c(t)$ which tries to reconstructs the original transmitted signal. The unipolar NRZ signal $y(t)$ is then sampled and used to recreate the original binary information signal by means of a decision device. The amplitude of each sample is compared with a pre-set threshold value. If the value is greater than the threshold value the output bit is 1 and if it is less the output bit is 0.

The output $y(t)$ of the receive filter is written as follows:

$$y(t) = \mu \sum_k a_k * p(t - KT_b) \tag{1.8}$$

Where μ is a scaling factor and $\mu p(t)$ is the scaled pulse and is obtained by convolving the impulse response of transmit filter $g(t)$, the impulse response of the channel $h(t)$ and the impulse response of the receive filter $c(t)$.

$$\mu p(t) = g(t) \circledast h(t) \circledast c(t) \tag{1.9}$$

where $\circledast$ denotes convolution. The receive filter output is then sampled at time $t_i = iT_b$ which gives

$$y(t_i) = \mu \sum_{k=-\infty}^{\infty} a_k p[(i-k)T_b] \tag{1.10}$$

$$y(t_i) = \mu a_i + \mu \sum_{\substack{k=-\infty \\ k \neq i}}^{\infty} a_k p[(i-k)T_b] \tag{1.11}$$

In the Equation (1.11), a_i denotes the required information signal and the second term represents the residual effect which leads to Inter-Symbol Interference during transmission.

The Equation (1.9) in the time domain can also be written in the frequency domain as follows:

$$\mu P(f) = G(f)H(f)C(f) \tag{1.12}$$

where $P(f), G(f), H(f)\ and\ C(f)$ are Fourier transforms of $p(t), g(t), h(t)\ and\ c(t)$ respectively.

In signal processing terms, rectangular pulses are transmitted through the transmit filter where a discrete Fourier transform is performed on these pulses. The Fourier transform of

a rectangular pulse is a sinc signal whose side lobes extend from -∞ to +∞. The side lobes close to the main lobe, also known as pre and post-main lobe tails contain important information required to reconstruct the signal. This signal is then passed through a channel and the receive filter which have a band limited frequency response similar to that of an ideal low pass filter. The side lobes of the sinc signal consequently get attenuated because of the band limitation. Due to lack of information caused by the attenuation of the side lobes, when an inverse Fourier transform is performed at the receive filter the output is distorted and this phenomenon is known as Inter-symbol Interference.

Nyquist proposed a criteria where if the response of the receive filter is as shown in Figure 1.7, then there will be no Inter-Symbol Interference in the received signal. The pulses are timed in such a way that the side lobe of the previous pulse will be zero when the magnitude of the next transmitted pulse is maximum. As a result of this the signal reconstructed at the receiver will be identical to the transmitted pulse.

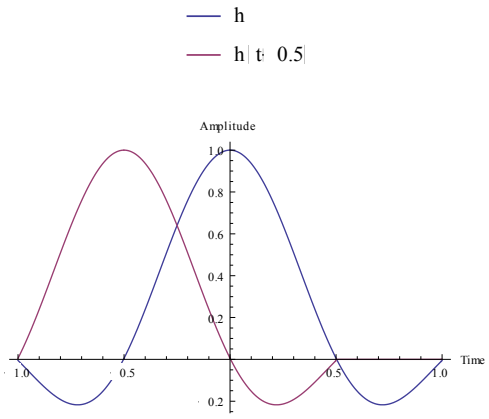

Figure 1.6. Received Pulse Shape in Time Domain with no Inter-Symbol Interference

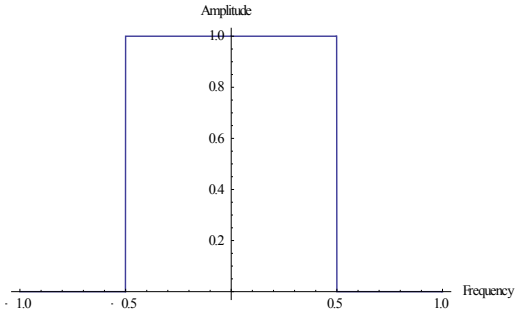

Figure 1.7. Frequency Response of Nyquist filter with Zero Inter-Symbol Interference

The sinc signal shown in Figure 1.6 can only be obtained if the response of the transmit filter is identical to that of an ideal low pass filter. But it is immensely complicated to fabricate a circuit to generate an ideal response. Furthermore, it is more likely that there will be timing errors in the sinc signal which can cause this theory to fail.

To avoid this a raised cosine filter could be used. A raised cosine filter is used to optimize the ideal low pass filter response by varying the steepness of the filter roll off. The filter response can be expressed as follows:

$$H(f) = \begin{cases} 1 & for\ |f| < 2W_0 - W \\ \cos^2\left(\frac{\pi}{4} * \frac{|f| + W - 2W_0}{W - W_0}\right) & for\ 2W_0 - W < |f| < W \\ 0 & for\ |f| < W \end{cases} \qquad (1.13)$$

where W is the absolute bandwidth and W_0 is the minimum Nyquist bandwidth for a rectangular spectrum and – 6db bandwidth for raised cosine spectrum. The roll-off factor represents the excess bandwidth as a fraction of W_0 which is given by $r = {(W - W_0)}/{W_0}$

where r = roll-off factor which lies in the range $0 \leq r \leq 1$.

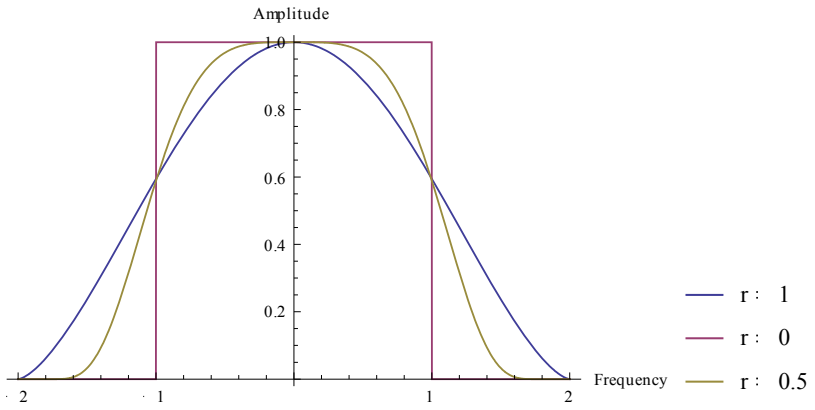

Figure 1.8. Frequency Response of a Raised Cosine Filter

Figure 1.8 illustrates the frequency response characteristics of a raised cosine filter. In this response the Nyquist minimum bandwidth for no inter-symbol interference $W_0 = 1$. The raised cosine filter allows excess bandwidth to be passed while keeping the amplitude of the side lobes for the sinc signal as small as possible. The smaller side lobe amplitude will mean lesser likelihood of errors caused by timing difference and will lead to reduced inter-symbol interference during transmission. But, a greater utilisation of bandwidth leads to a requirement of greater revenue for the telecommunication service provider. Although the raised cosine filters can be realised physically, the major disadvantage that plagues this filter is the excess amount of bandwidth required to be transmitted with the information pulses. This major disadvantage can be avoided with the help of a filter design which takes advantage of Linear Prolate Functions and its various useful properties.

1.4. Objectives

1. To simulate a filter designed using linear prolate functions in Mathematica which can provide highly accurate reconstruction of a rectangular pulse after filtering.
2. To compare signal reconstruction capabilities of a prolate filter with those of an ideal low pass filter.
3. To improve performance of the prolate filter by varying the threshold value ‘M’ of the filter.
4. To verify if a prolate filter can be used as an anti-aliasing filter.

1.5. Outline of the Thesis

This thesis is divided into seven chapters. Chapter 1 introduces the problem of Inter-Symbol Interference present in a baseband transmission system. It also provides information about traditional methods used for reducing the interference. It also provides details on the research problem and objectives of this thesis. Chapter 2 provides an overview of Linear Prolate Functions and its various advantageous properties. The time-bandwidth concentration problem and its similarity with problems in quantum mechanics is also discussed. Chapter 3 presents a review of important literature which provides significant contextual information regarding the basic theory used to solve the Inter-Symbol Interference problem in the system. Chapter 4 describes and confirms the theory used for creation of a prolate filter for reducing the interference problem and some results simulating the sampling theorem are also detailed. Additionally, it also provides a brief introduction of a software used for simulating the filter, known as Mathematica. Chapter 5, details the application of the prolate filter i.e. in a baseband receiver for reducing Inter-Symbol Interference and in a baseband transmitter for anti-aliasing. Moreover, further variations of the prolate filter are also illustrated. Chapter 6 provides concluding remarks which summarizes the major advantages and outcomes of this research. Additionally, potential applications of the prolate filter in other fields are suggested.

CHAPTER 2: LINEAR PROLATE FUNCTIONS

The previous chapter has provided details on the inter-symbol interference problem. It can be seen that the current methods also have a basic flaw of requiring additional bandwidth to reduce interference in the signal. The filter mentioned earlier of reducing inter-symbol interference was designed using Linear Prolate Functions. This chapter introduces Linear Prolate Functions and its various advantageous properties. It also describes the similarity between the time-bandwidth concentration problem in signal processing field with a problem in quantum mechanics field described by Heisenberg's uncertainty principle.

It is a well-known fact that there is an inverse relationship between Time and Frequency. A small instant in time leads to infinitely long bandwidth in the frequency domain. Every physical device has a band-limited response which causes its output to undergo severe attenuation if a high frequency signal is applied at its input. This band-limiting nature of the device gets in the way of successfully reconstructing a signal. If a signal is confined to a specific interval or band in both time and frequency domain, it can be exactly reconstructed after transmission. But, there are no signals currently present which are maximally enclosed in a specific time interval and frequency band. This conundrum of simultaneously confining the signal and its amplitude spectrum has been present for a long time in digital communication; specifically signal processing.

In terms of Quantum Mechanics the confining problem can be expressed by Heisenberg's Uncertainty Principle. It simply states that certain physical properties of an entity are

complementary. For example, if the position of some particle is accurately known then it becomes difficult to accurately predict the momentum of said particle. Gabor was the first one to relate this theory to signal or information processing. He was able to make this hypothesis because there is an apparent duality between particles and waves. Consider a signal $r(t)$ having unit energy [5] such that

$$\int_{-\infty}^{\infty} r^2(t)dt = \int_{-\infty}^{\infty} |R(f)|^2 \, df = 1 \tag{2.1}$$

Gabor-Heisenberg's uncertainty principle thus can be expressed mathematically [5] as follows:

$$\sigma_r{}^2 \sigma_R{}^2 \geq \frac{1}{(4\pi)^2} \tag{2.2}$$

where $r^2(t)\ and\ |R(f)|^2$ can be considered as probability densities and $\sigma_r\ and\ \sigma_R$ are their corresponding variances. From the expression above the inverse relationship between variances of time and frequency can be clearly seen.

Mathematically speaking, a meaningful measure of concentration for a signal $r(t)$ can be seen in equation (2.3) [5]:

$$\alpha^2(T) = \frac{\int_{-T/2}^{T/2} r^2(t)dt}{\int_{-\infty}^{\infty} r^2(t)dt} \tag{2.3}$$

If $r(t)$ is time-limited in equation (2.3) from $(-T/2\ to\ T/2)$ then $\alpha^2(t)$ will have a maximum value of unity. But because of the inverse relationship, the band-limiting of a

signal will not allow it to be time-limited. Hence, to solve the problem of obtaining a unity value for $\alpha^2(t)$ while keeping $r(t)$ band-limited, was undertaken by three scientists from Bell laboratories namely; H. Pollak, H. Landau, and D. Slepian which lead them to develop a set of band-limited functions that were maximally concentrated in a given time interval. These functions are known as Prolate Spheroidal Wave Functions.

The Helmholtz wave equation for steady waves is given by [6],

$$(\nabla^2 + k^2)\psi = 0 \tag{2.4}$$

$where\ k = \frac{2\pi}{\lambda}, \lambda = wavelength,$

The solution for the wave equation in spheroidal co-ordinates can be found by using three different ordinary differential equations as shown below [6]:

$$\frac{d}{dt}\left[(1-t^2)\frac{dS(c,t)}{dt}\right] + \left[A - c^2t^2 - \frac{m^2}{1-t^2}\right]S(c,t) = 0 \tag{2.5}$$

$$\frac{d}{d\xi}\left[(\xi^2-1)\frac{dR(c,\xi)}{d\xi}\right] - \left[A - c^2\xi^2 + \frac{m^2}{\xi^2-1}\right]R(c,\xi) = 0 \tag{2.6}$$

$$\frac{d^2\Phi(\varphi)}{d\varphi} + m^2\Phi(\varphi) = 0 \tag{2.7}$$

where S is the angular component, R is the radial component and Φ is the azimuthal component. By solving Equation (2.5) and Equation (2.6) we get two kinds of solutions for radial and angular components namely $R^1_{mn}(c,\xi), R^2_{mn}(c,\xi), S^1_{mn}(c,t), S^2_{mn}(c,t)$. The

azimuthal solution is not required for determining prolate functions and hence will not be considered in this thesis. The angular and radial solutions of the first kind are used to determine prolate spheroidal wave functions. Alternatively, the second kind solutions are required for the oblate case which will not be taken into consideration in this thesis. By considering $m = 0$ the prolate spheroidal angular function $S_{0n}^{1}(c,t)$ can be used to compute a set of functions having many advantageous properties over trigonometric functions which are extensively used. Therefore, a one dimensional prolate spheroidal wave function can be termed as a Linear Prolate Function designated by $\psi_n(c,t)$. Similarly, the prolate spheroidal radial function $R_{0n}^{1}(c,1)$ can be used to determine the corresponding linear prolate eigenvalues designated by $\lambda_n(c)$. Mathematically, linear prolate functions and their corresponding eigenvalues are expressed as follows [7] [8] [9]:

$$\psi_n(c,t) = \frac{\sqrt{\lambda_n(c)/t_0}}{\sqrt{\int_{-1}^{1}(S_{0n}(c,t))^2\,dt}} * S_{0n}\left(c,\frac{t}{t_0}\right), \tag{2.8}$$

$$\lambda_n(c) = \frac{2c}{\pi}[R_{0n}(c,1)^2] \tag{2.9}$$

2.1. Mathematical Notations

Different researchers have used different notations and normalizations for the prolate spheroidal wave functions. In this thesis the mathematical notations and normalizations are similar to those used by Flammer [10] and Slepian [7]. As seen in Figure 2.1, linear prolate functions $\psi_n(c,t)$ are dependent on four factors [11]: the time parameter t, the time-limited interval t_0, the order of the function n, and the space bandwidth product parameter c. The bandwidth parameter $c = t_0\Omega_0$,

$where\ \Omega_0$ is the finite bandwidth to be considered.

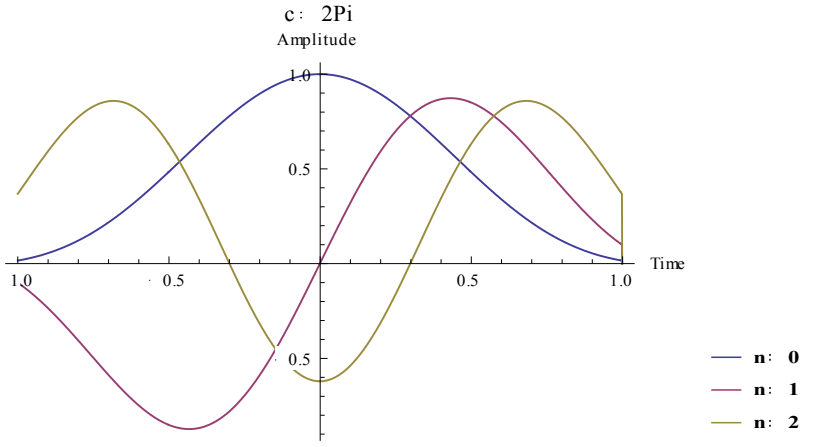

Figure 2.1. Linear Prolate Functions of different orders

It is important to note that both the linear prolate functions ψ_n and their eigenvalues λ_n are dependent on space bandwidth product parameter 'c'. The significance of this parameter can be understood by considering a Fourier transform on a rectangular pulse obtained by using the usual trigonometric functions. The width of the main lobe of the sinc pulse obtained from the operation is determined by the width of the rectangular pulse. There is no other free parameter which can vary this width which proves to be practically disadvantageous. On the other hand, if a Fourier transform is performed on a rectangular

pulse created by using linear prolate functions the space-bandwidth parameter ‘c’ can be used to vary the width of the main lobe of the sinc pulse. Similar to Slepian’s literature the parameter ‘c’ will not be specifically stated in further expressions, with the awareness that all the prolate quantities are dependent on c. The space-bandwidth parameter is an extra advantageous parameter provided by linear prolate functions which will be studied in detail in the results. Furthermore in this thesis, the interval under consideration t_0 will always be from $-1 < t_0 < 1$.

2.2. Important Properties of Linear Prolate Functions

Linear Prolate functions have some important properties which will be detailed in this section. The following properties were first proposed by Slepian and Pollak in [7] and were discussed analytically in detail by Frieden in [8]. This research has further proved these properties with simulated results in Mathematica software as shown below:

- Linear Prolate functions are invariant to finite or infinite Fourier transform:

$$\int_{-x_0}^{x_0} \psi_n(x)\, e^{j\omega x}\, dx = j^n\, (2\pi\lambda_n x_0/\Omega)^{\frac{1}{2}}\, \psi_n(\omega x_0/\Omega) \tag{2.10}$$

In the expression above the left hand side denotes the Fourier transform of the prolate function and the right hand side is a scaled version of the same prolate function with a constant multiplier. It can be clearly seen that the finite Fourier transform of the prolate function is proportional to the same prolate function. The analytical result above can also be proved by simulation as follows:

Consider a linear prolate function ψ_{20} as shown in Figure 2.2

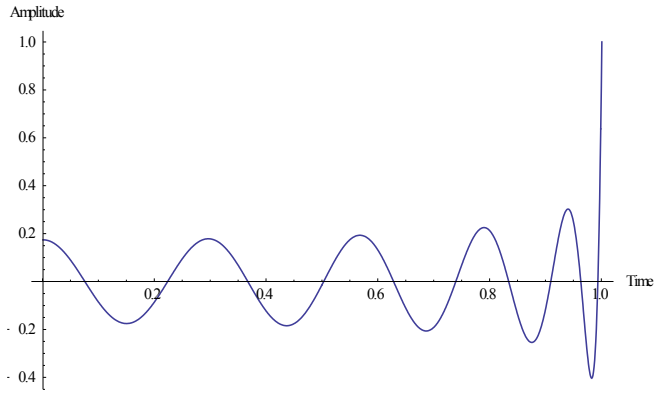

Figure 2.2. Linear Prolate Function with order n = 20

In this case the prolate function is even symmetric so only the positive half of the signal is shown. The negative half of this signal will be the exact mirror image of Figure 2.2. After performing Fourier transform we get the following result

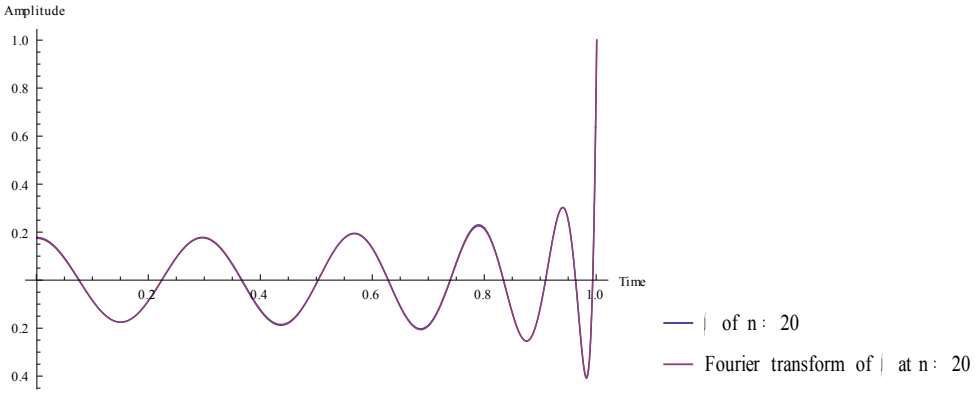

Figure 2.3. Fourier Transform of a Prolate Function

It is observed from Figure 2.3 that the Fourier transform follows ψ_{20} exactly. Furthermore, by carrying out an infinite Fourier transform on equation (2.10) it can be seen that these prolate functions are also invariant to the infinite Fourier transform:

$$\int_{-\infty}^{\infty} \psi_n(x)\, e^{-j\omega x}\, dx = \begin{cases} j^{-n}\,(2\pi x_0/\Omega\lambda_n)^{\frac{1}{2}}\,\psi_n\left(\dfrac{x_0\omega}{\Omega}\right), for\ |\omega| \le \Omega \\ 0, \qquad\qquad\qquad\qquad for\ |\omega| > \Omega \end{cases} \tag{2.11}$$

Although there are certain functions such as $e^{-\pi x^2}, |x|^{-1/2}\ and\ \text{sech}(\pi x)$ which are invariant to an infinite Fourier transform, only prolate functions have the property to be invariant to a finite Fourier transform. Most of the following properties were formed as a result of Fourier transform property of prolate functions.

- Eigenvalues λ_n are also eigenvalues of a sinc kernel

  In matrix theory, λ is said to be an eigenvalue of a function if it satisfies the following equation [12]:

$$A\,v = \lambda\,v \tag{2.12}$$

  where v is a non-zero vector known as an Eigen function. The special property of an Eigen function is that the eigenvector only gets scaled, even when any operation is performed on it by a matrix. Alternatively, most vectors get scaled and rotated by most matrix operations [12]. In case of prolate functions by taking a finite Fourier transform of equation (2.10),

$$\int_{-x_0}^{x_0} \psi_n(x)\,\frac{\sin\Omega(y-x)}{\pi\,(y-x)}\,dx \;=\; \lambda_n\,\psi_n(y) \tag{2.13}$$

  it is evident that the result as seen in equation (2.13) satisfies the general equation for eigenvalues and eigen functions. In this way, λ can also be considered as an eigenvalue for a sinc kernel as the eigen function.

- Linear Prolate functions are complete and orthonormal in a finite interval and orthogonal over an infinite interval:

  In number theory, real numbers are considered to be complete as they have no missing terms between two numbers. Alternatively, rational numbers are considered incomplete since irrational numbers are present between rational numbers. Trigonometric functions such as $sin(x)$ and $cos(x)$ are orthogonal and complete only over a finite interval. On the other hand, linear prolate functions are orthogonal and complete over an infinite and finite interval:

$$\int_{-\infty}^{\infty} \psi_m(x) * \psi_n(x)\, dx = \begin{cases} 0, & for\ m \neq n \\ 1, & for\ m = n \end{cases} \tag{2.14}$$

$$\int_{-x_0}^{x_0} \psi_m(x) * \psi_n(x)\, dx = \begin{cases} 0, & for\ m \neq n \\ \lambda_n, & for\ m = n \end{cases} \tag{2.15}$$

  Mathematically, the completeness property can be confirmed as follows [8]:

  It is understood from (2.11) that the linear prolate functions are band-limited over an infinite interval. If a band-limited function $f(x)$ is given, it can be expanded using prolate functions using the expression seen in equation (2.16):

$$f(x) = \sum_{n=0}^{\infty} a_n\, \psi_n(x) \tag{2.16}$$

  Using equation (2.14), the coefficient a_n can be expanded as follows:

$$a_n = \int_{-\infty}^{\infty} f(y)\, \psi_n(y)\, dy \tag{2.17}$$

Substituting this a_n back into equation (2.16) and exchanging the orders of summation and integration, we get:

$$f(x) = \int_{-\infty}^{\infty} f(y)\, dy \sum_{n=0}^{\infty} \psi_n(y)\, \psi_n(x) \tag{2.18}$$

Multiplying equation (2.16) with $\psi_m(x)$ and integrating on both sides over a finite interval $|x| \leq x_0$ and by using orthonormality property of prolate functions in a finite interval given by equation (2.15), we get:

$$a_n = \frac{1}{\lambda_n} \int_{-x_0}^{x_0} f(x)\, \psi_n(x)\, dx \tag{2.19}$$

Using equation (2.13), equation (2.16), and equation (2.19), we can prove that:

$$\sum_{n=0}^{\infty} \psi_n(y)\, \psi_n(x) = \pi^{-1}\Omega\, sinc\Omega(y - x) \tag{2.20}$$

Therefore, substituting equation (2.20) into equation (2.18), we get,

$$f(x) = \pi^{-1}\Omega \int_{-\infty}^{\infty} f(y)\, sinc\Omega(y - x)\, dy \tag{2.21}$$

Equation (2.21) is similar to a proven mathematical property which states that a band-limited function is its own sinc transform. This proves that the series provided in equation (2.16) converges to the required band-limited function $f(x)$ and that the prolate functions are complete on an infinite interval.

- Extrapolation property of Linear prolate functions

Eigenvalues λ_n of prolate functions are an infinite scalar set of real positive numbers obeying the following relation:

$$1 \geq \lambda_0 > \lambda_1 > \lambda_2 > \ldots > 0 \tag{2.22}$$

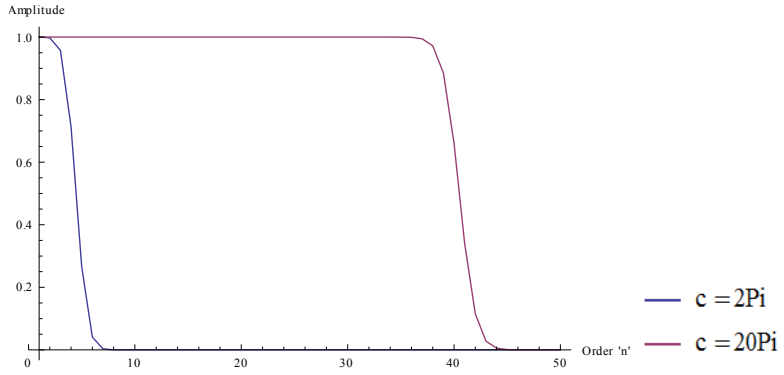

Figure 2.4. Progressively decreasing eigenvalues for increasing order 'n'

Dividing equation (2.15) by equation (2.14), we get:

$$\lambda_n = \frac{\int_{-x_0}^{x_0} [\psi_n(x)]^2 \, dx}{\int_{-\infty}^{\infty} [\psi_n(x)]^2 \, dx} \tag{2.23}$$

Equation (2.23) clearly shows that λ_n measures the energy content of the linear prolate function in the interval. From Figure 2.4, for a fixed 'c' value the eigenvalues λ_n can be seen to reduce slightly from unity value until their order reaches a critical value given by:

$$n_{crit} = \frac{2c}{\pi} \tag{2.24}$$

After this critical value λ_n rapidly approaches zero but never truly reaches zero value. Furthermore, in terms of energy it can be seen that as the value of order 'n'

is increased the energy content of the prolate function moves outside the interval under consideration i.e. $[-1,1]$. Thus, the prolate function has an inherent extrapolation property with which the behaviour of the function everywhere with infinite limits can be predicted if the behaviour of the same function in band limited form is known over a finite interval. Mathematically an extrapolation formula can be derived by substituting equation (2.19) into equation (2.16):

$$f(x) = \sum_{n=0}^{\infty} {\lambda_n}^{-1}\, \psi_n(x) \int_{-x_0}^{x_0} f(x')\, \psi_n(x')\, dx' \tag{2.25}$$

The prolate filter extensively makes use of this extrapolation property for reducing inter-symbol interference.

- Linear Prolate Functions are symmetric and they have exactly 'n' zeros in the interval $\pm t_0$

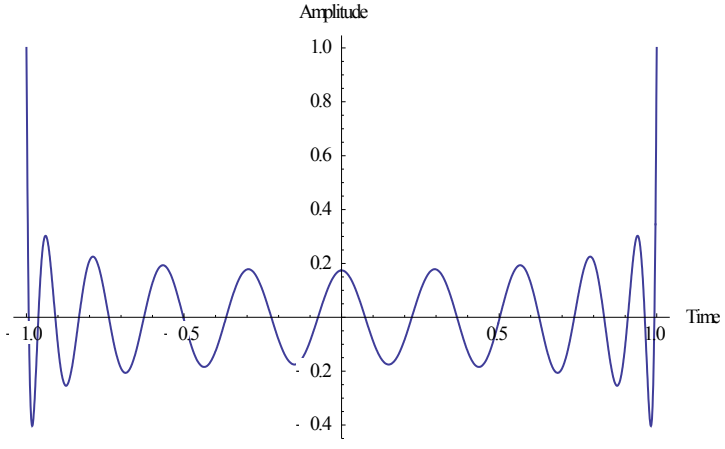

Figure 2.5. Entire Prolate Function ψ_{20}

From Figure 2.5, it is observed that the prolate functions are symmetric in the interval t_0 under consideration. Additionally, the number of zero crossings are

exactly equal to the order ‘n’ of the linear prolate function. In this case there are 20 zero crossings since the order $n = 20$.

It is evident from Figure 2.5 that a linear prolate function is time-limited. The Fourier transform property states that the Fourier transform of a linear prolate function is a scaled version of the prolate function itself. Hence, it can be stated that the prolate function is band-limited as well. In this way, the prolate functions are able to solve the time-bandwidth concentration in the signal processing field.

CHAPTER 3: BACKGROUND INFORMATION

In the previous chapter, the time-bandwidth concentration problem present in signal processing was solved by making use of linear prolate functions and its properties. In this chapter, the resolution problem in optics will be shown to be similar to the inter-symbol interference problem in baseband communication. Furthermore, some background information will be provided which helps in understanding the different techniques used by researchers to solve the resolution problem in optics.

In the field of digital communication due to the band limited nature of the filter, the pulses transmitted through the channel expand outward and interfere with each other. The interference known as inter-symbol interference makes it difficult to obtain an accurate signal reconstruction at the receiver of a baseband communication system. A similar limitation can be seen in the resolving power of optical systems such as microscopes or telescopes. In imaging systems, each point being projected on a screen is expected to have a Dirac Delta response. However due to diffraction, the delta response stretches outwards and a pattern similar to a sinc function in two dimensions is obtained. The sinc function pattern in two dimensions appears as an airy disk with a main lobe or disk having maximum intensity and the side lobes of the sinc functions appear as surrounding disks with reducing luminous intensity. If two such airy disks are brought close to each other, it becomes demanding to isolate them. In other words, the resolving capability of the system is affected. Similar to Nyquist criteria, the lower limit for resolving two points projected on a screen as separate was provided by Rayleigh criterion. According to this criterion two points are considered to be resolved when the principal maximum of one of disk coincides

with the first minimum of the other [13]. According to the Rayleigh criterion a limit can be obtained at which an imaging system, such as a microscope is just able to resolve the two point as separate entities. This limit is as follows:

$$d = 0.61 \frac{\lambda_0}{n \sin\theta} \tag{3.1}$$

where λ_0 is the wavelength of light in vacuum and $n \sin\theta$ is also known as the Numerical Aperture of the imaging system. For an imaging system, the numerical aperture describes the 'light gathering power' [13] i.e. the different angles over which the system can accept light. In this case, the illumination will be incoherent and the aperture will be circular.

It is evident that the resolution problem in optics field is similar to the inter-symbol interference problem in digital communication field. Hence, the methodologies used for solving the resolution problem in optics can also be used to solve the inter-symbol interference problem. The best way to solve the resolution problem will be to reduce the width of the Airy disk or main maxima created by the point source thereby increasing resolution beyond Rayleigh limit. But this creates a detrimental effect of increase in brightness of the rings surrounding the main maxima. Several researchers in photonics field have tried to overcome this limitation with varying results. The methodologies used by different researchers and their disadvantages are detailed in the subsequent section.

The theory of reducing the main maxima width to increase the resolution was obtained from the field of microwave theory. After the introduction of microwave techniques researchers were looking into ways to obtain highly directional antennas. Schelkunoff [14] proposed that the amplitude of the signal radiated by a linear end fire array antenna of 'n' elements can be represented by a polynomial:

$$A_0 + A_1 \exp[i\psi] + A_2 \exp[2i\psi] + \cdots + A_{n-1} \exp[(n-1)i\psi] = A_0 + A_1 z + A_2 z^2 + \cdots + A_{n-1} z^{n-1} \tag{3.2}$$

where A_0, A_1 are complex amplitudes and $\psi = \frac{2\pi l}{\lambda}$, where l is the spacing between elements of the antenna. In the complex plane for a uniform array, its zeroes are equispaced along the entire unit circle but Schelkunoff was able to show a remarkable increase in directivity by keeping the zeroes inside the unit circle corresponding to $\cos(\theta) \leq 1$.

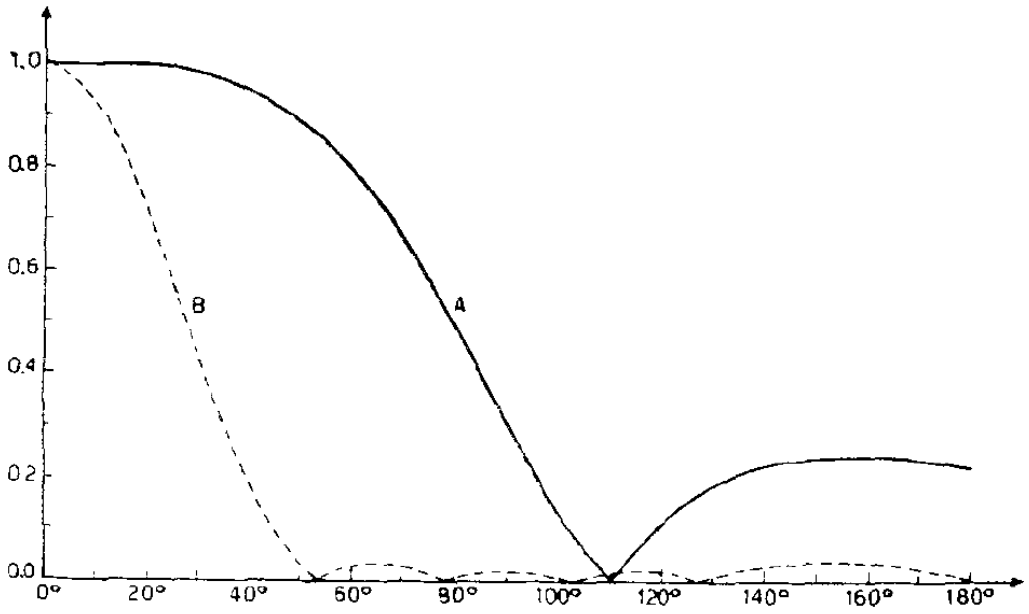

Figure 3.1. Directive properties of two end fire antenna arrays with $l = \lambda/8$ [15].

In Figure 3.1, the curve A denotes the radiation pattern of a uniform array while curve B denotes highly directive antenna array due to zeroes being equispaced inside the unit circle. Although this theory was revolutionary at that time, it was difficult to implement this theory practically as there would be immense reactive currents generated by this antenna array.

G. Toraldo Di Francia [15] understood the theory and translated it into optical terms. According to him diffracted rays are actually evanescent waves which get attenuated along a direction perpendicular to the pupil. A uniform antenna array has its zero's or cones of silence spaced out equally in the region of radiating waves ($\cos(\theta) \leq 1$) and in the region of evanescent waves ($\cos(\theta) > 1$). Schelkunoff in his theory has removed the zeros from the evanescent region and transferred them into the radiating region. Due to this, the power wasted in the side lobes has been reduced while leaving the power transmitted in the main

lobe intact, thereby increasing the total directivity of the antenna. Similarly, in order to solve the optical problem G. Francia removed the rings surrounding the central maxima up to the region of evanescent waves or in practical terms outside the field of the instrument as shown in Figure 3.2:

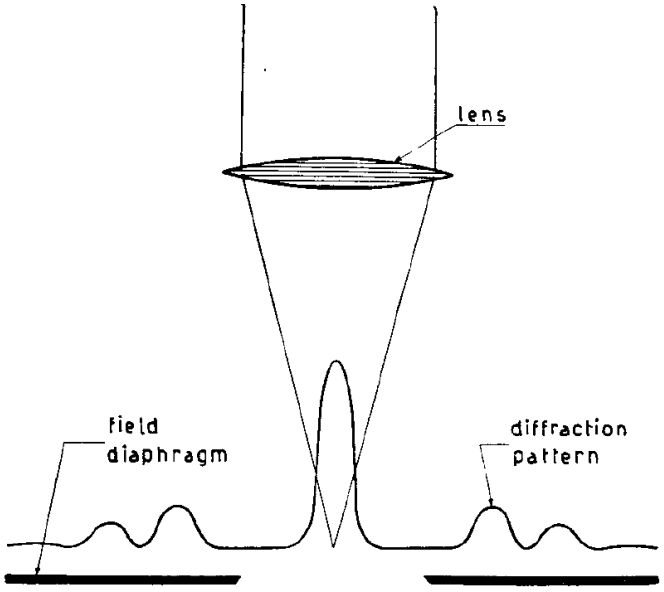

Figure 3.2. Stretching the luminous rings outside field of the instrument [15]

He achieved this by making use of ring apertures of different diameters. Although this method achieved the desired objective of increase in resolution, a major disadvantage of this method was that large amount of luminous flux would be wasted in the ring aperture structure if higher reduction in the ring diameter was required. It was thus observed that the efficiency of this method was very poor.

H. Osterberg and J. Wilkins [16] [17] have described a new approach to reduce the maxima of the Airy disk. Instead of using bulky ring apertures, they suggested to apply a coating to

the exit pupil such that it will reduce the diameter of the Airy disk and the rings surrounding the maxima will have low luminous intensity.

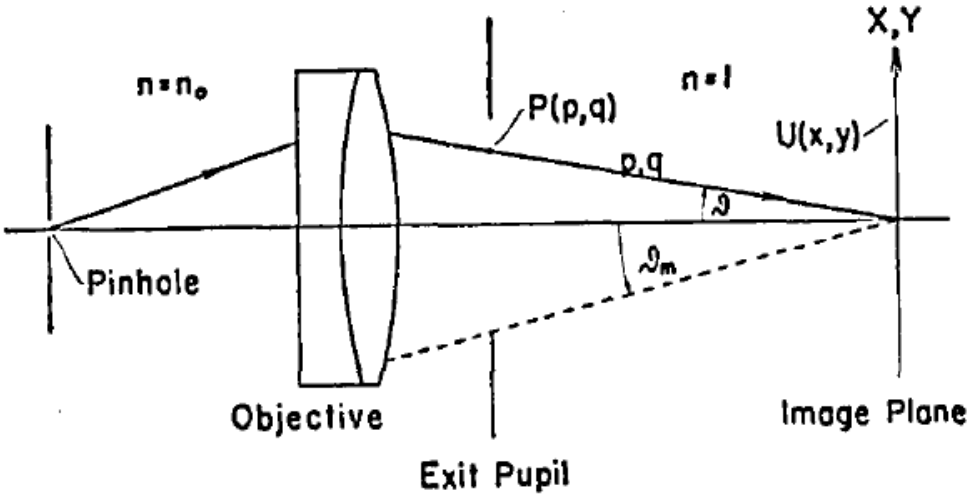

Figure 3.3. An Optical System [16]

This coating will alter both the amplitude and phase distribution of the diffraction pattern over the exit pupil. They deduced that such a coating could be obtained by expressing the diffraction pattern over the exit pupil as a series of Sonine Integrals. Each series of Sonine integrals had a unique coating function which described the amplitude and phase information of the refracting material which was to be coated on the exit pupil. In [16], they have presented results for a coating which only aims to reduce the radius of the central maxima of the Airy disk.

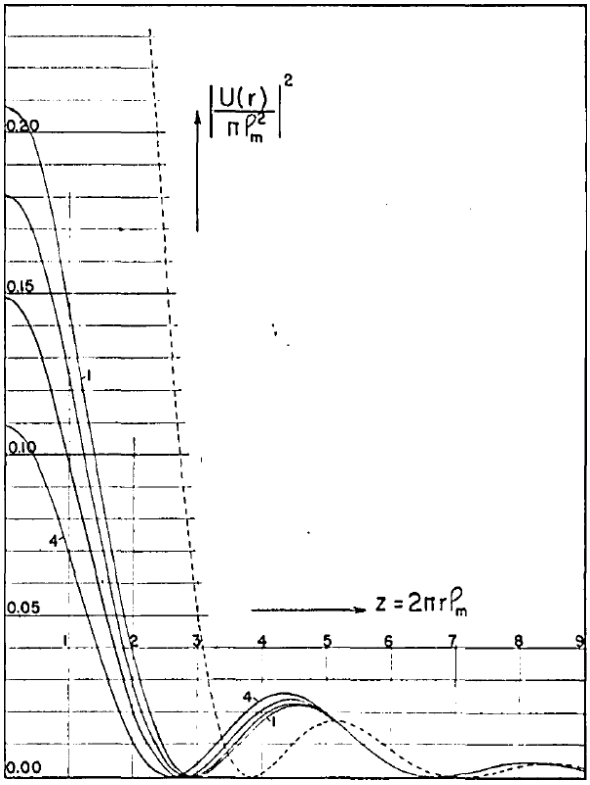

Figure 3.4. Comparison of four Sonine type Diffraction curves [16]

In Figure 3.4, the dotted curve is the one observed for uncoated diffraction while the other 4 curves are obtained by using a coating derived from Sonine Integrals. Even though the size of the maxima has reduced, the intensity of the maxima has also reduced which is unfavourable for the optical system. In [17], J. Wilkins has tried to negate this problem and increase the intensity of the maxima.

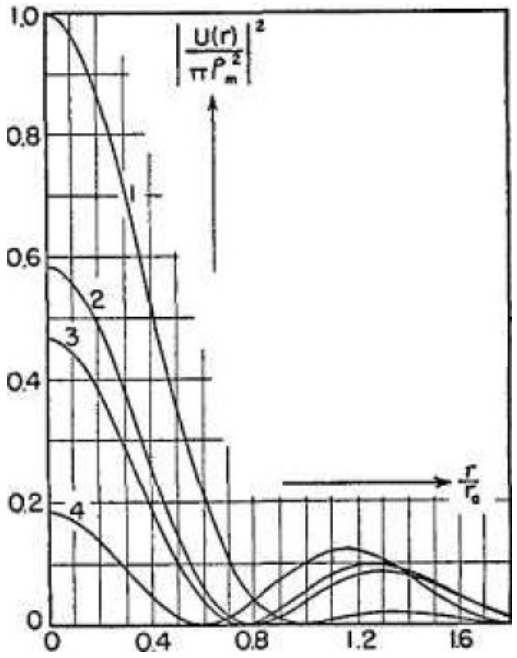

Figure 3.5. Diffraction pattern of varying radii of central maxima of Airy disk [17]

Even though, the intensity of the maxima has increased as compared to Figure 3.4, it is still less than the intensity obtained for the uncoated diffraction pattern as seen in curve 1 in Figure 3.5. The limitation present in this theory is mainly due to finite scanning aperture.

J. Harris in [18] has provided two important conclusions through his findings. Firstly, he has made use of the identity theorem or uniqueness theorem which states that for an absolute resolution limit to exist, the two objects need to have identical spectral frequencies within the pass band of the optical system and non-identical spectral frequencies outside the pass band. As two objects cannot have the same spectra (images), he concluded that limited precision is the only major factor limiting the resolving power of the system. This limit is determined by noise present in the system. He also stated that if the frequency spectra of an object within the pass band of an optical system is known, then it can be used

to determine the spectrum of the object beyond the pass band of the optical system. Finally, he also utilized the sampling theorem in the frequency domain to show the mathematical nature of a spatially bounded object. An object having finite dimensions can be defined completely using the Fourier series. He derived a formula relating the frequency spectrum $G(f_x, f_y)$ with the Fourier coefficients G_{mn}. The expression is as follows:

$$G(f_x, f_y) = XY \sum_{m=-\infty}^{\infty} \sum_{n=-\infty}^{\infty} G_{mn} \frac{\sin \pi[\left(\frac{m}{X}\right) - f_x]X}{\pi[\left(\frac{m}{X}\right) - f_x]X} * \frac{\sin \pi[\left(\frac{m}{Y}\right) - f_y]Y}{\pi[\left(\frac{m}{Y}\right) - f_y]Y} \tag{3.3}$$

Thus, by extrapolating the Fourier spectrum and taking the inverse Fourier transform, an image can be obtained which has more detail as compared to the original image, due to the increase in resolution.

C. Barnes in [19] was the first one to effectively make use of prolate functions in object restoration procedure. He stated that any imaging system can be characterized by a linear integral operation

$$b(\xi) = \int g(\xi, x) * a(x) dx \tag{3.4}$$

where $b(\xi)$ is the complex amplitude of the image and $a(x)$ is the complex amplitude of the object and $g(\xi, x)$ is the imaging kernel or the point amplitude response. By making use of various favourable properties of prolate functions, he concluded that by increasing the order 'N' of the prolate functions the response of the image kernel becomes more like a Dirac Delta function:

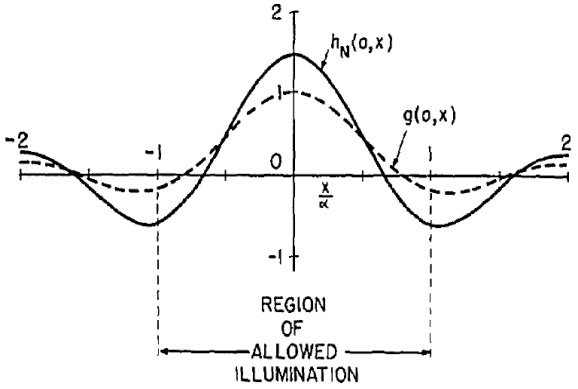

Figure 3.6. Point response of an imaging system using prolate functions N = 2

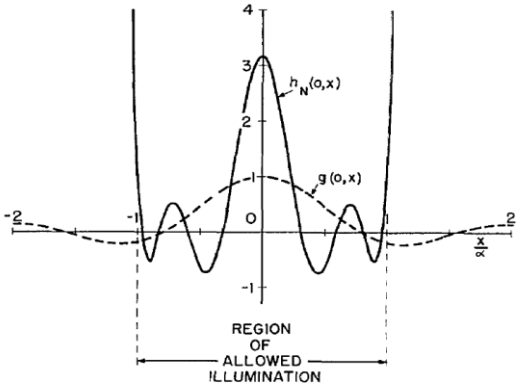

Figure 3.7. Point Response of an imaging system using prolate functions N = 8

In Figure 3.6 and Figure 3.7, the dotted line is the point response of an ordinary imaging system without the use of prolate functions. The main aim in such type of object restoration procedure is to have a point response as narrow as possible. A fine point amplitude response will provide a higher resolution which will increase the amount of detail in the image. This increase in detail will provide a sharper and visually better restored image. Although, the procedure suggested by Barnes solved the illumination problem present in the works of Osterberg and Wilkins, it still had its limitations. The point response outside the range $(-1,1)$ becomes extremely large as we increase the order 'N' of the prolate functions (to obtain a perfect Dirac delta response). In practice, to obtain a perfect response, great care has to be taken not to allow any stray light to be present.

In this way, several researchers have used various techniques to solve the resolution problem. But each method explained previously has a drawback which was solved by Frieden in [8] which will explained in the next chapter.

CHAPTER 4: IMPLEMENTATION

In this chapter the theory used to develop the filter algorithm by Frieden, which overcomes all of the previously mentioned limitations will be explained. Additionally, the theory will also be verified by comparing the results of Frieden with simulated results obtained in the Mathematica software package. The sampling theorem which was detailed in Chapter 1:, was simulated in Mathematica software and its results are presented in this chapter. Furthermore, some basic concepts of interpolation which is the most important step in the filter algorithm will also be detailed.

4.1. Basic Theory

B. Frieden [8] combined the different methodologies mentioned previously in the review of literature and fashioned a theory which has solved most of the shortcomings in the work done previously by various researchers. He used linear prolate functions to construct a point amplitude response whose side-lobes do not increase in size even when the order 'n' of the prolate function is increased. It is known that the Fourier transform of a unity function is a Dirac Delta function. But this statement is not true if a finite Fourier transform is used. Thus, we can say that there are no functions available today whose finite Fourier transform is a Delta function. However, with the help of linear prolate functions we can obtain a function whose finite Fourier transform can provide a Dirac delta function up to a finite extent.

Therefore, we need a function which has the following property:

$$\int_{-\Omega}^{\Omega} d\omega\, U(\omega)\, \cdot e^{j\omega x} = \delta(x)\ \ for\ |x| \leq\ x_0 \tag{4.1}$$

Since $U(\omega)$ is only defined over a finite interval $|\omega| \leq \Omega$, equation (4.1) can also be written as

$$U(\omega) = \sum_{n\,=\,0}^{\infty} a_n\ \cdot\ \psi_n(\omega x_0/\Omega)\ \ for\ |\omega| \leq\ \Omega \tag{4.2}$$

Substituting equation (4.2) back into equation (4.1) we find that coefficient a_n is needed to satisfy

$$(2\pi\Omega/x_0)^{\,1/2} \sum_{n\,=\,0}^{\infty} j^n\, {\lambda_n}^{1/2}\ a_n\, \psi_n(x) = \delta(x)\, for\ |x| \leq\ x_0 \tag{4.3}$$

The completeness and orthogonality property of linear prolate functions as seen in equation (2.15) can also be written as follows:

$$\sum_{n\,=\,0}^{\infty} {\lambda_n}^{-1}\, \psi_n(0)\, \psi_n(x) = \delta(x)\ \ for\ |x| \leq\ x_0 \tag{4.4}$$

By comparing equation (4.3) and equation (4.4) we can find coefficient a_n

$$a_n = (x_0/2\pi\Omega)^{(1/2)}\, j^{-n}\, {\lambda_n}^{-3/2}\, \psi_n(0) \tag{4.5}$$

Substituting a_n from equation (4.5) back into equation (4.2)

$$\mathrm{U_M}(\omega) = (\mathrm{x_0}/2\pi\Omega)^{(1/2)} \sum_{\mathrm{n\ (even)\,=\,0}}^{\mathrm{M}} (-1)^{\mathrm{n}/2} {\lambda_\mathrm{n}}^{-3/2} \psi_\mathrm{n}(0) \psi_\mathrm{n}(\omega \mathrm{x_0}/\Omega) \tag{4.6}$$

In order to evaluate equation (4.6) in practice, the upper limit of the summation was changed from ∞ to M. 'M' indicates the maximum number of terms required to get the required response. In the rest of this thesis 'M' will be referred to as the threshold value. In optics, the function $U_{40}(\omega)$ is also known as the Pupil function. A Pupil function indicates how a light wave is affected as it travels through an optical imaging system such as a camera or a microscope. The function $U_{40}(\omega)$ obtained in the frequency domain is as follows:

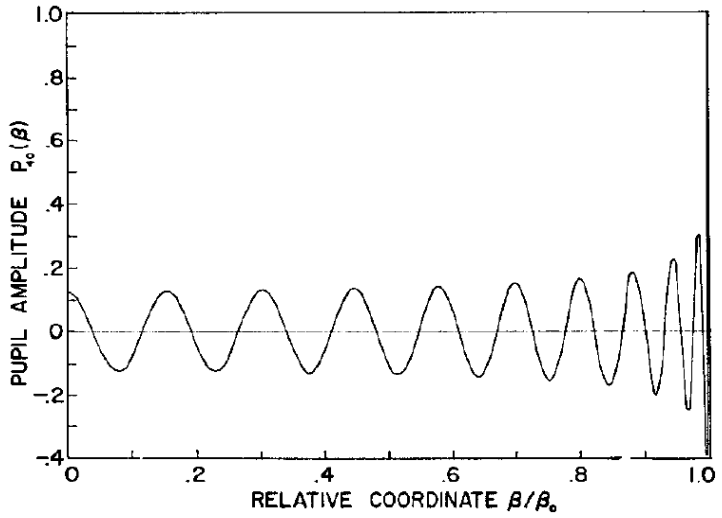

Figure 4.1. Pupil Function for M = 40 [20]

The inverse Fourier transform of the pupil function provides the required Dirac delta function as seen in equation (4.7) and the response it generates is as seen in Figure 4.2:

$$\delta_M(x) = \sum_{n=0}^{M} \lambda_n^{-1}\ \psi_n(0)\ \psi_n(x) \tag{4.7}$$

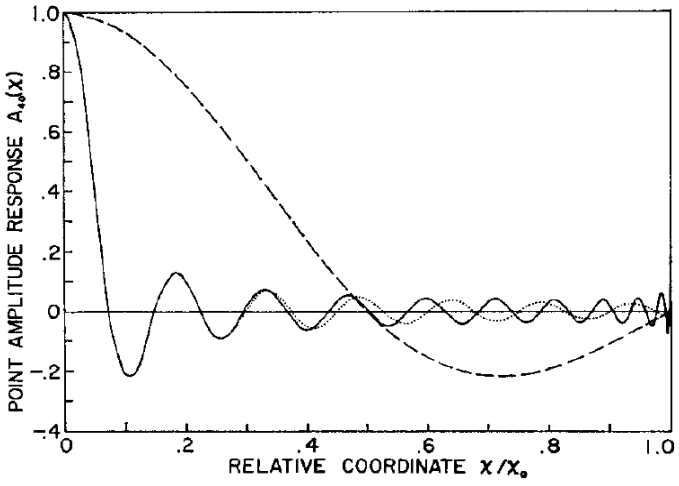

Figure 4.2. Point Amplitude response of pupil function for M = 40 and for an uncoated aperture [20]

In Figure 4.2, the dotted curve is the point amplitude response from an uncoated aperture while the solid curve is obtained from the inverse Fourier transform of the pupil function with a threshold value of M = 40. The response denoted by the solid curve can be improved by increasing the threshold value in equation (4.6).

4.2. Interpolation

Interpolation was an important step required in the algorithm for implementing inverse Discrete Fourier transform with high precision and accuracy. The idea for using interpolation while maintaining high precision of the values before integration was obtained from a concept proposed by A. Devasia and M. Cada in [21]. In [21], a piecewise polynomial interpolation is used to calculate the overlap integral with high precision. It is well understood that two points form a straight line. To be exact, these two points define a polynomial of a certain degree (one in case of two points) whose graph passes through these two points. In the same way 'n' number of points can define a specific ordered polynomial given by:

$$p_n = a_0 + a_1 x^1 + a_2 x^2 + a_3 x^3 + \cdots + a_n x^n \tag{4.8}$$

where 'n' denotes the number of coefficients as well as the order of the interpolating polynomial. In this way, the entire time interval for a linear prolate function between $[-1,1]$ which contains 2001 samples is divided into 8 segments i.e. each segment contains 251 samples of the scalar product contained within the overlap interval. A piecewise polynomial interpolation as seen in (4.8) is applied on each of these samples due to which a polynomial of high order is obtained which is then integrated to obtain the required overlap integral [21]. The sampling process provides the user with points which describes the behavior of the function over a time period. In most cases while simulating continuous data with discrete data points, interpolation is used on the known values so that a value in between these known values can be found. This value approximates the behavior of the function between those two points most accurately. There are different types of

interpolations defined in the literature. Due to the simplification of the numerical analysis, the amount of interpolation error depends upon the interpolation type and the data used. Papoulis in [22] has provided some important conclusions regarding the problem of estimating errors arising from simplification of various numerical operations involving band limited signals. He states that the maximum value of the interpolation error can be minimized only by properly selecting the interpolation coefficients.

In this case Hermite Interpolation is used as it provides the desired high accuracy due to which the inverse Fourier transform is possible. In this type of interpolation, first order derivatives are also used to provide a better approximation of the function. The interpolation error when Hermite interpolation is used depends on the space between two data points. Thus a major disadvantage observed in this interpolation type is, when higher order polynomials are used the interpolation starts to exhibit oscillatory behavior near the end points.

4.3. Implementation Using Mathematica

In this thesis, the entire theory was implemented on a software package known as Mathematica version 9.0. Mathematica is a type of computational software which utilizes symbolic mathematics for calculation and analysis purposes. It was invented by Stephen Wolfram and is developed by Wolfram Research of Champaign, Illinois. The reasons why Mathematica was used are as follows:

- Mathematica provides a very high accuracy for any results obtained through various operations as compared to other universally used commercial software such as Matlab, C++ or Java.
- In order to perform higher order calculations such as summation or integration multiple times, other software requires construction of various functions and loops but in Mathematica the same thing can be done with relative ease with the help of a single command.
- Automatic translation of English language into Wolfram code.
- Support for complex numbers, interval arithmetic and symbolic computation.
- Tools for parallel programming.

For the implementation of B. Frieden's theory to be successful the prolate functions had to be calculated to a very high accuracy. Machine accuracy is of only 15 digits meaning that after the decimal point only 15 digits are considered correct or significant, while the remaining digits are wrong or insignificant. This limited accuracy was a major reason why researchers in the past have not been able to use prolate functions effectively in various applications. Dr. Michael Cada was able to successfully implement prolate functions in

Mathematica with a very high accuracy of 200 digits. In previous literature the researchers have only been able to use c (space bandwidth product parameter) values up to 40, but with very low accuracy. However, with the help of a proprietary algorithm developed by Dr. Cada the c values up to 200π or higher can be easily defined with very high accuracy. In this thesis three c values namely 2π, 10π, and 20π were used for modelling of the prolate filter in Mathematica. Furthermore, all the different input signals for the algorithm were generated by making use of highly accurate linear prolate functions.

Initially the linear prolate filter was designed in Mathematica. Its time domain response obtained from an inverse Fourier transform was then compared with the time domain response of an ideal low pass filter with bandwidth $\pm 2\pi$. The low pass filter can be generated using linear prolate functions as seen in equation (4.9):

$$f(x) = \sum_{n\,(even)\,=\,0}^{M} (-1)^{n/2}\, \lambda_n{}^{(-\frac{1}{2})}\, \psi_n(0)\, \psi_n(\omega x_0/\Omega) \tag{4.9}$$

where all the prolate functions and eigenvalues are dependent on $c = 2\pi$. The response is seen in Figure 4.3:

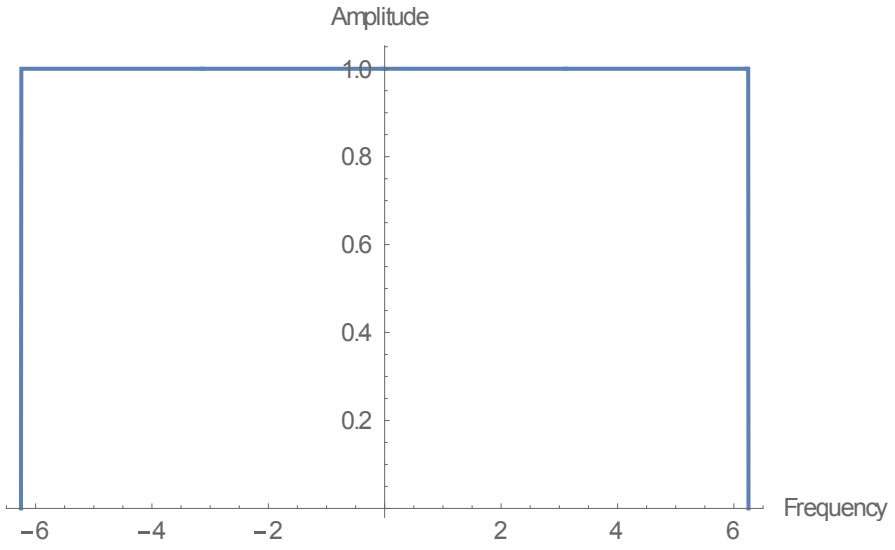

Figure 4.3. Frequency domain response of an ideal low pass filter

The time domain response of the ideal filter can be obtained by an inverse Fourier transform as seen in Figure 4.4.

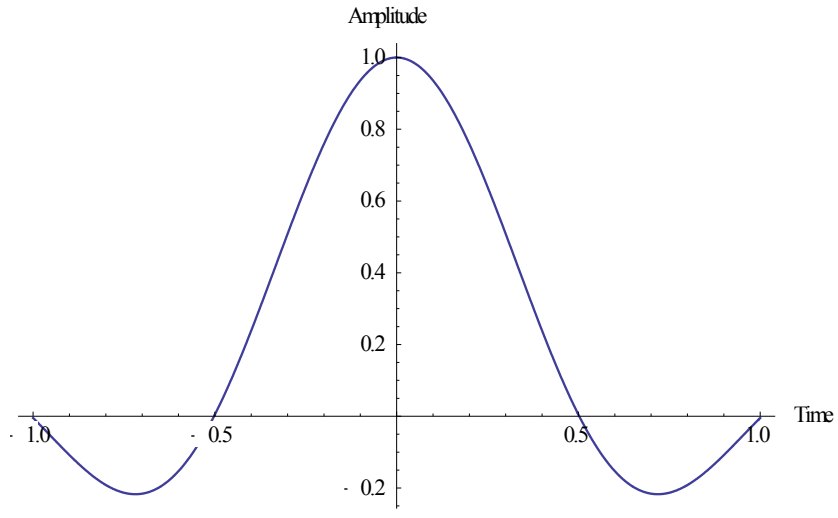

Figure 4.4. Time Domain Response of an ideal Low pass filter

The frequency domain response of the prolate filter is obtained from equation (4.6). The corresponding frequency and time domain response plots for the prolate filter are as seen in Figure 4.5 and Figure 4.6 respectively:

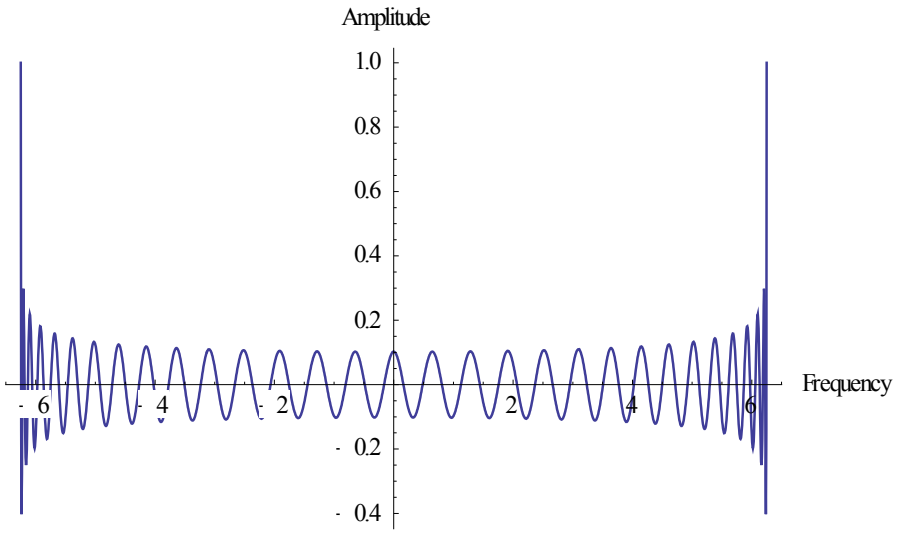

Figure 4.5. Frequency Domain Response of Prolate filter with M = 60

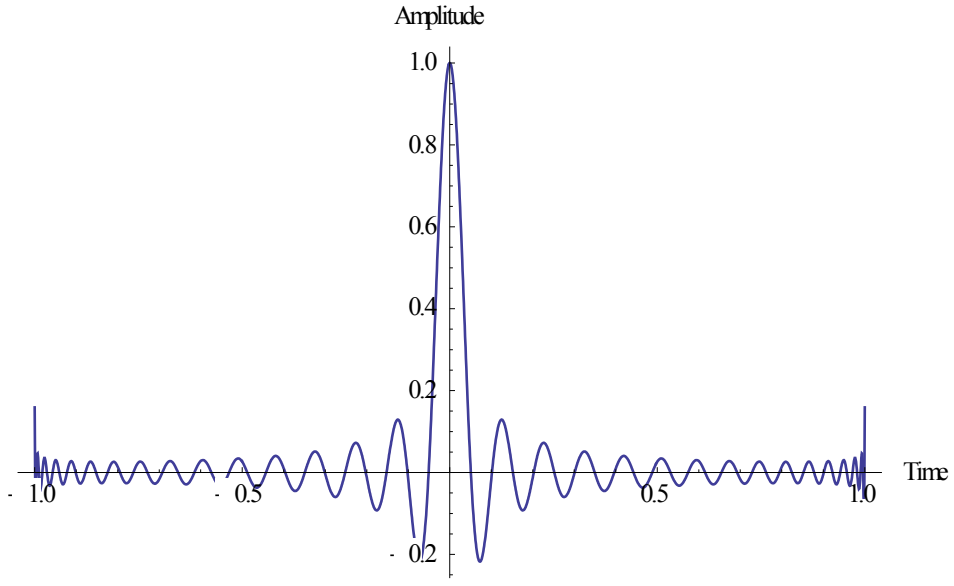

Figure 4.6. Time Domain Response of Prolate Filter with M = 60

The response obtained in Figure 4.6 from a prolate filter can also be obtained from the ideal low pass filter if the bandwidth of the filter is increased. But this increase in bandwidth leads to several limitations which will be explained in the results and discussion chapter.

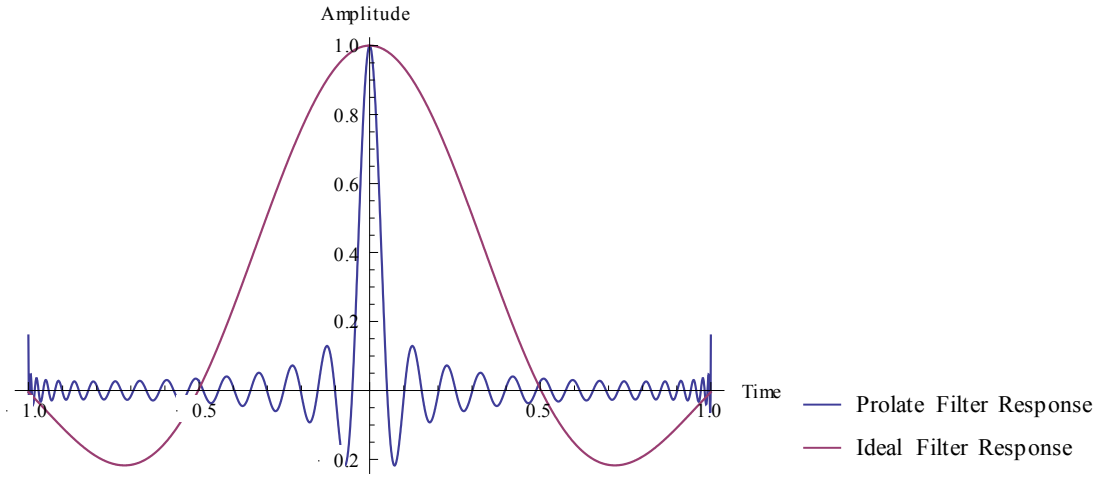

Figure 4.7. Comparison of time domain response of ideal filter with prolate filter

In Figure 4.7, by comparing the two time domain plots it can be clearly seen that the prolate filter has artificially increased the bandwidth of the low pass filter which provides an increased resolution in the time domain response. This response can be improved further by increasing the threshold value 'M'. Furthermore, the total increase in resolution can be defined by equation (4.10) [8].

$$\delta_M \approx \frac{3c}{M\pi} \tag{4.10}$$

where c is the space bandwidth product parameter and M is the threshold value of the pupil function in equation (4.6). δ_M in the equation (4.10) indicates the approximate width of the main lobe of the sinc signal obtained after performing inverse Fourier transform on the prolate filter. In this case, for $M = 60$ the core width is approximately 0.1.

4.4. Implementation of Sampling Theorem in Mathematica

According to sampling theorem, the phenomena of aliasing occurs in a signal if the signal is sampled at a frequency less than twice the Nyquist frequency. Nyquist frequency as stated in Chapter 1:, is equal to the maximum frequency of the input signal. Hence, in order to verify if a prolate filter can be used as an antialiasing filter, the sampling theorem must first be simulated so that the Nyquist frequency can be obtained from the simulation. All of the signals used for the simulation are obtained by making use of prolate functions with a Slepian frequency of $c = 2\pi$.

The input signal used for implementing sampling theorem in Mathematica is as shown in Figure 4.8:

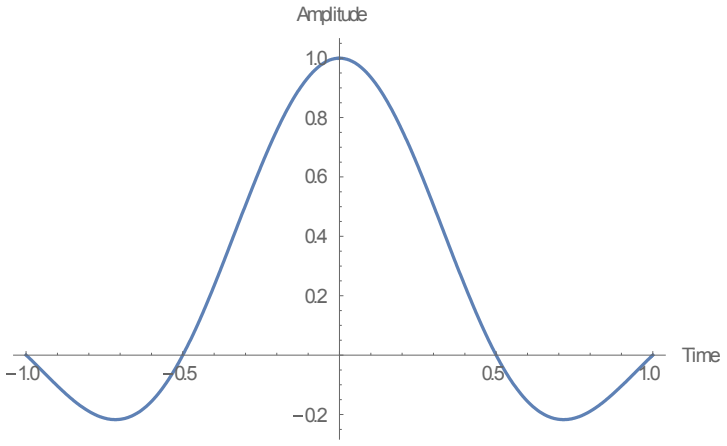

Figure 4.8. Input Signal in the Time Domain

The frequency domain response of the input signal to determine the maximum frequency of the input signal is as shown in Figure 4.9:

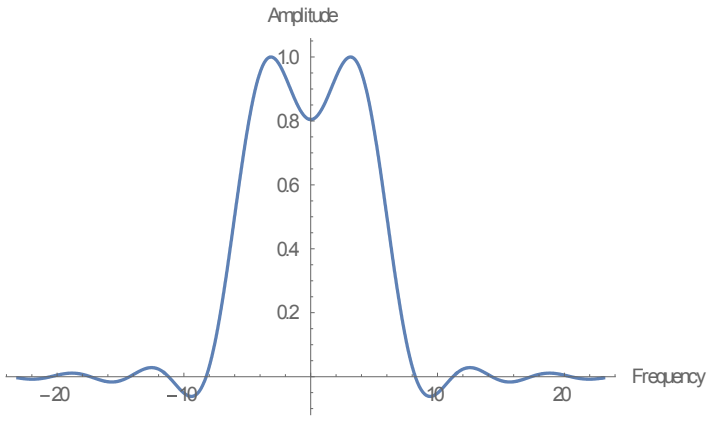

Figure 4.9. Frequency Domain Response of the Input Signal

The maximum frequency of the input signal is $f_N = 8\ Hz$. Hence, in order to avoid aliasing in the signal the sampling frequency should be greater than 16Hz. The input signal was initially sampled by a train of impulses with a sampling frequency $f_s = 25.78\ Hz$ as shown in Figure 4.10:

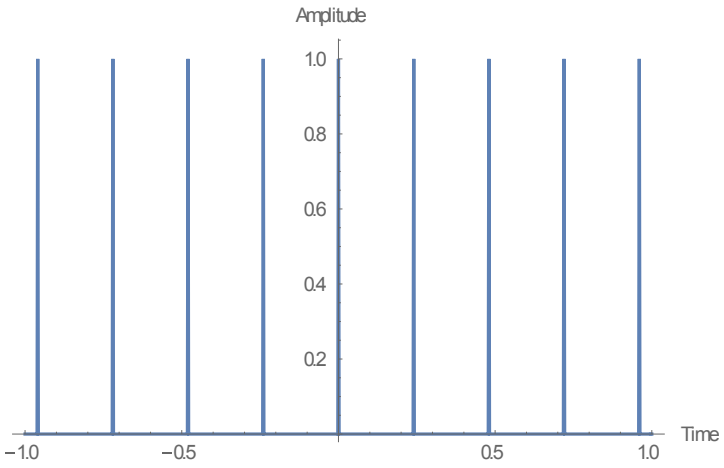

Figure 4.10. Train of Impulses with sampling frequency $f_s = 25.78\ Hz$

The effect of aliasing can be easily observed from the Frequency domain hence the sampled signal is converted to the frequency domain by using a Fourier transform. As the sampling

frequency is greater than twice the maximum frequency of the input signal i.e. $f_s > 2f_N$, no aliasing is obtained in the frequency domain of the signal as seen in Figure 4.12:

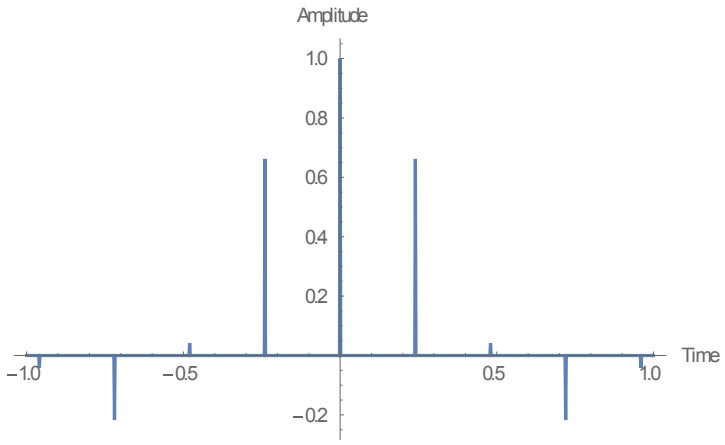

Figure 4.11. Time Domain Response of the Resultant Signal

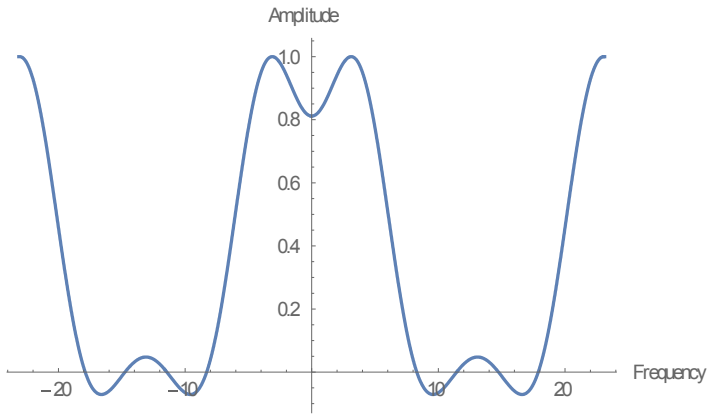

Figure 4.12. Frequency Domain Response of the Resultant Signal

The input signal was then sampled by a train of impulses with a sampling frequency less than twice the maximum frequency of the input signal i.e. $f_s < 2f_N$ which is as seen in Figure 4.13:

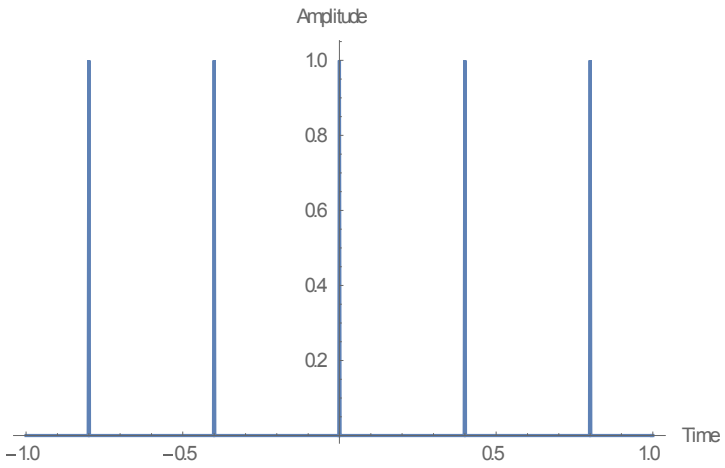

Figure 4.13. Train of Impulses with sampling frequency $f_s = 16.20\ Hz$

The frequency domain response of the resultant sampled signal is as seen in Figure 4.14:

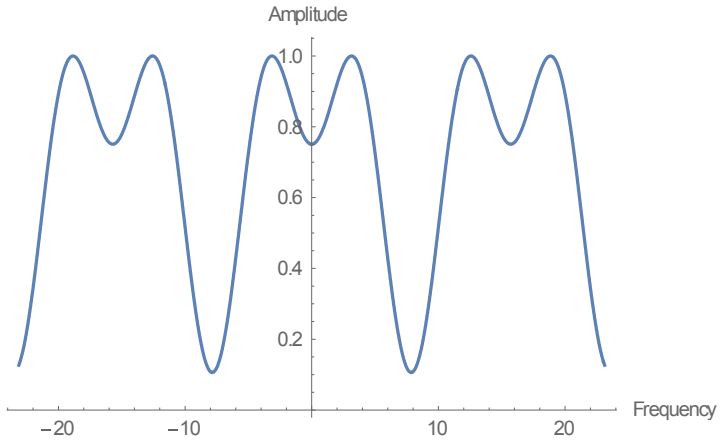

Figure 4.14. Frequency Domain Response of the Resultant Sampled Signal

As $f_s < 2f_N$, aliasing occurs in the signal which is an undesirable effect as it complicates the reconstruction of the signal at the receiver.

Thus, the sampling theorem was implemented in Mathematica and the Nyquist rate for an input signal was calculated. Furthermore, Frieden's methodology for reducing the width of the main lobe while keeping the amplitude of the side lobes to a minimum was successfully

implemented in Mathematica software. The highly accurate linear prolate functions was the main feature added to this research. The major advantage of using highly accurate linear prolate functions is that higher values of order ‘n’ and higher c values can be obtained with ease. The calculated Nyquist frequency will be used to verify, if a prolate filter can be used as an antialiasing filter which will be seen in the next chapter. The different results, obtained by using the prolate filter in the receiver of a baseband transmission system for various c values, will also be detailed in the next chapter.

CHAPTER 5: RESULTS AND DISCUSSION

In the previous chapter B. Frieden's theory of super-resolving pupils and the sampling theorem was successfully implemented in Mathematica. This chapter will be divided into three main sections. Firstly, the results of using prolate filter at the receiver side of a baseband communication system will be detailed. Secondly, the results of a simulation used to verify if a prolate filter can be used as an anti-aliasing filter will also be described. Finally, the effects of varying different important parameters of the prolate filter on the output of the receiver will also be shown.

5.1. Application of the prolate filter in a Baseband Receiver

In this section Frieden's theory discussed in the previous chapter will be used to solve a major limitation in the digital communication field. In a nutshell, the prolate filter will be used to reduce the inter-symbol interference in a digital communication system. In the field of digital communication, baseband transmission of information pulses is severely affected by Inter-symbol interference which occurs because of the band limited nature of the filters and it causes the apparent widening of the pulses after travelling through the communication channel.

Figure 5.1. A Communication Channel

Consider a simple communication channel as seen in Figure 5.1 where an information signal with data bits 1001 is generated by the transmitter: The data which is initially

generated at the transmitter is converted into rectangular pulses for transmission as seen in Figure 5.2.

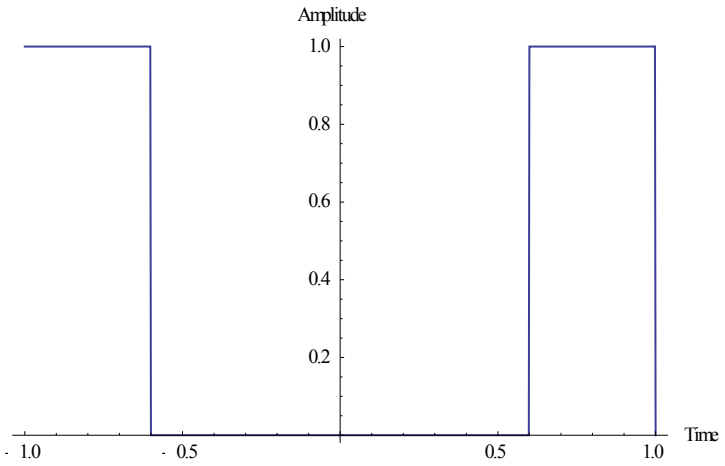

Figure 5.2. Transmitted Digital Signal

In signal processing for calculating the output of any system, time domain analysis using convolution can be extremely complex and time consuming. Hence, in order to simplify the calculations, a frequency domain analysis is considered by performing a Fourier transform operation on the input signal as seen in Figure 5.3:

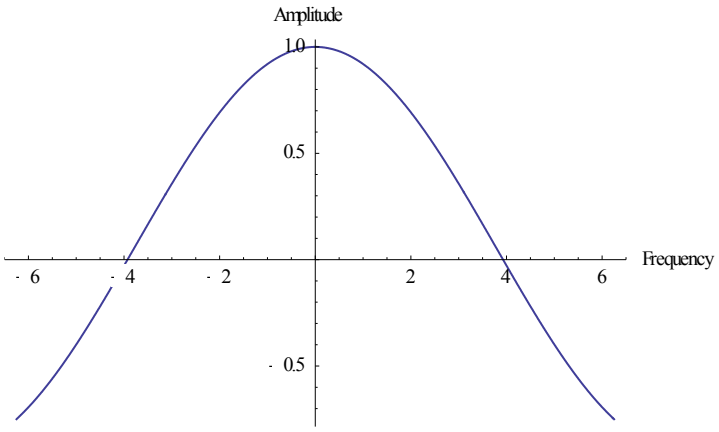

Figure 5.3. Fourier Transform of the Transmitted Signal

Any communication channel generally adds noise to the transmitted signal which can be removed at the receiver with a low pass filter. Inter-symbol interference due to bandwidth limitation is the major issue considered in this thesis. Hence, the bandwidth under consideration i.e. $\pm 2\pi$ of the channel is considered noiseless.

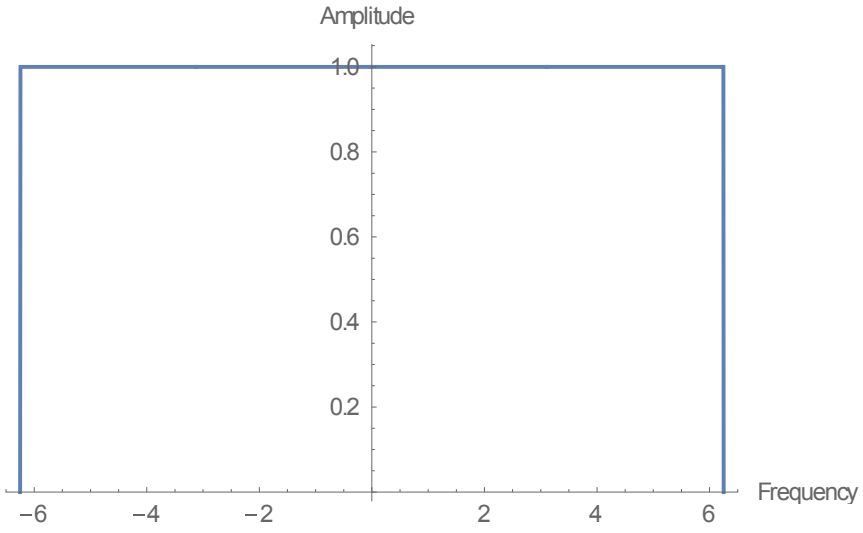

Figure 5.4. Frequency Response of an ideal low pass filter at the receiver

Since frequency domain analysis is used, the input signal at the receiver will be the product of the Fourier transform of the transmitted signal multiplied by the frequency response of

the filter at the receiver as seen in Figure 5.4. With the aim of obtaining the information signal back in the time domain at the output, an inverse Fourier Transform operation is performed. But due to the band-limited response of the filter, side-lobes of the sinc signal which contain valuable information for signal reconstruction are lost. The reconstruction of the information signal is severally affected because of this as seen in Figure 5.5:

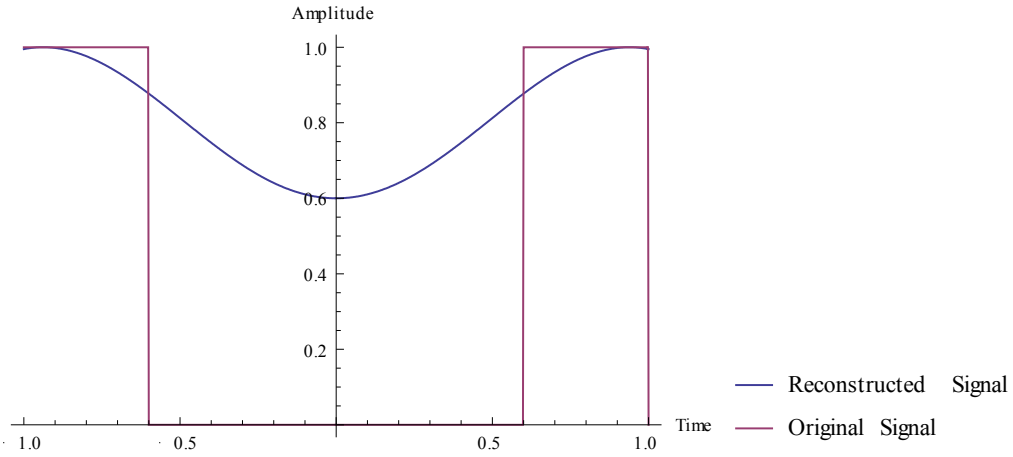

Figure 5.5. Reconstructed Signal using Ideal Low pass Filter

The reconstruction of the signal can be vastly improved by expanding the bandwidth of the low pass filter at the receiver. The reconstructed signal obtained by expanding the bandwidth of the low pass filter is as seen in Figure 5.6:

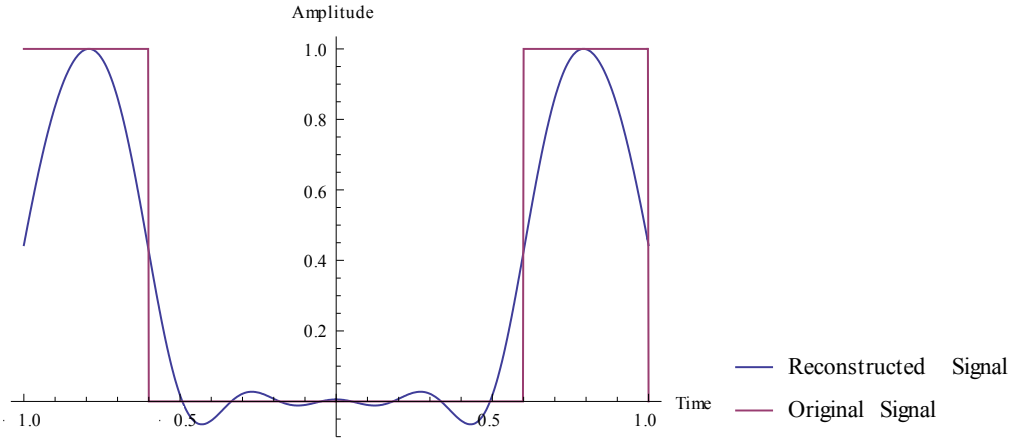

Figure 5.6. Reconstructed Signal Using a filter with increased bandwidth

There are several factors which limit this expansion of bandwidth in the filter. Firstly, if the bandwidth of the filter is increased further it increases the high frequency noise in the signal which defeats the major purpose of a low pass filter. Secondly, the increase in bandwidth also increases the amount of losses in the hardware circuit used to realize the filter in physical form. Moreover, the increase in bandwidth also leads to a phenomenon known as Skin effect where the electrical signals passing through the wires travel towards the edge of the wire. This increases the amount of losses in the system and also decreases the signal to noise ratio. This can be avoided by increasing the tolerance levels of the components but it causes the components to become more bulky which is unfavorable for a communication system.

In order to overcome these limitations of physically increasing the bandwidth of the filter, one can increase the bandwidth artificially by making use of a prolate filter. The response equation of the prolate filter in question is as seen in equation (4.6) and the response it generates is as seen in Figure 5.7. The bandwidth range of the prolate filter in this case is from -2π to $+2\pi$.

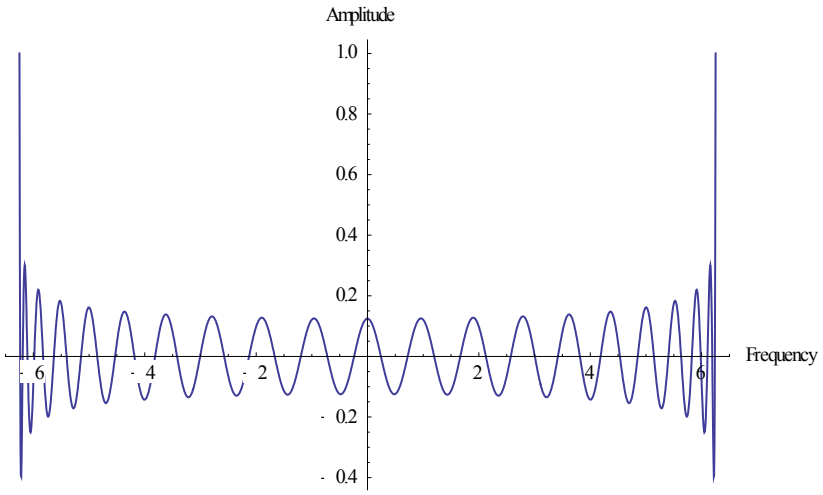

Figure 5.7. Frequency Response of a Prolate Filter with order M = 40

The reconstructed signal obtained by using a prolate filter is as seen in Figure 5.8 and is the same as the one obtained by physically increasing the bandwidth of the filter as seen in Figure 5.6.

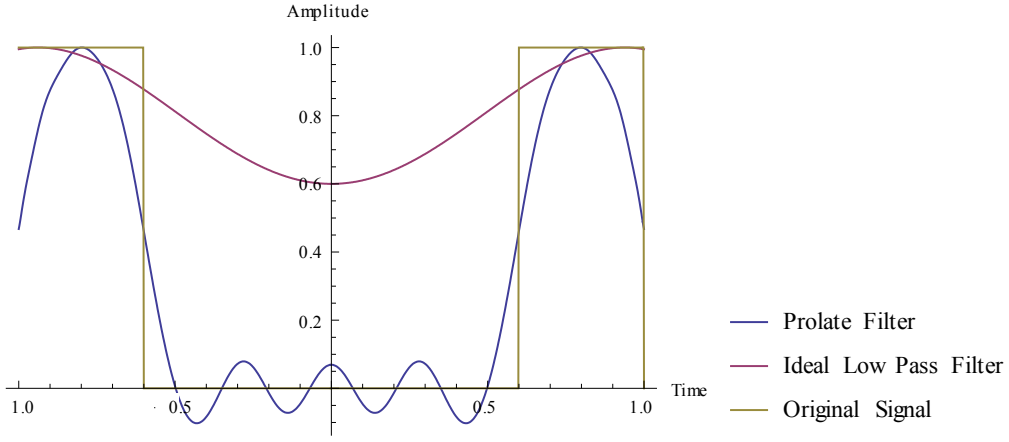

Figure 5.8. Reconstructed Signal using prolate filter with M = 40

The response of the prolate filter can be improved further by increasing the threshold value 'M' in equation (4.10) as seen in Figure 5.9.

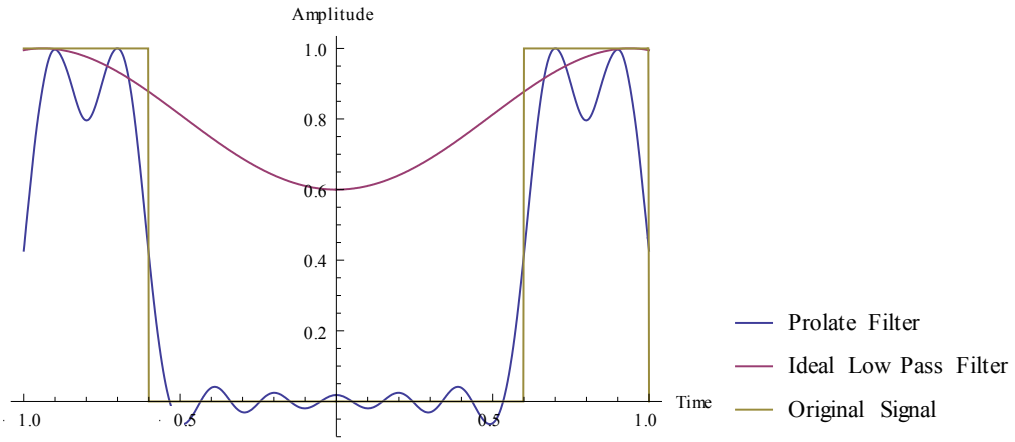

Figure 5.9. Reconstructed Signal using prolate filter with M = 60

It can be seen from Figure 5.10 and Figure 5.11 that the prolate filter successfully reduces inter-symbol interference in a system even when the input information signal is changed.

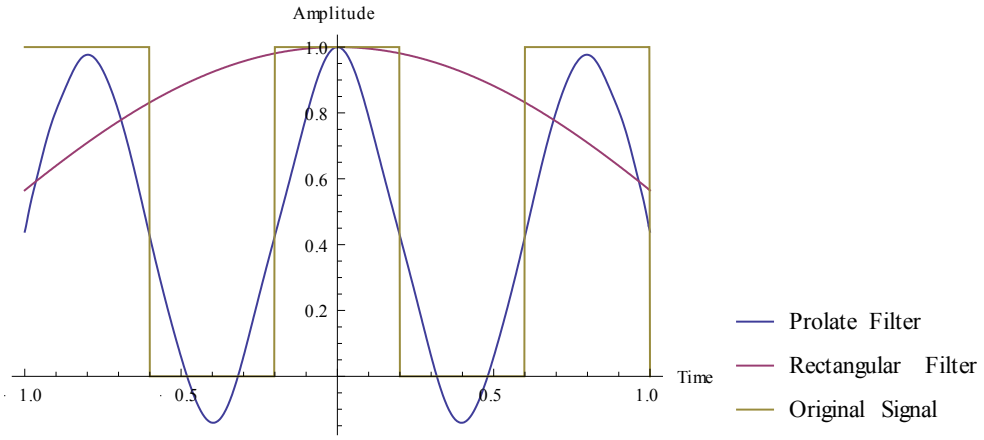

Figure 5.10. Reconstructed Signal obtained from Data Signal – 1001001 with maximum order M = 40.

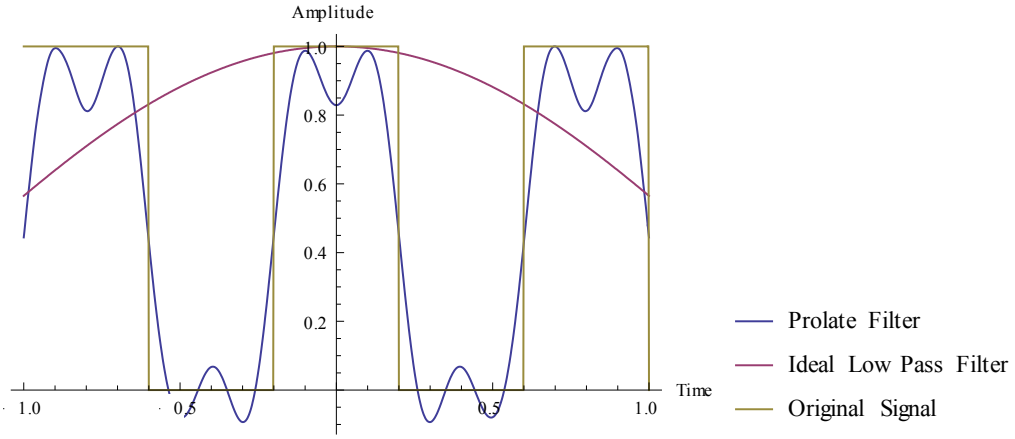

Figure 5.11. Reconstructed Signal obtained from Data Signal – 1001001 with maximum order M = 60.

5.2. Application of the prolate filter in a Baseband transmitter

An anti-aliasing filter is a filter used to reduce the undesirable phenomena of aliasing from the input signal. The anti-aliasing filter can be used before sampling the signal (pre-filtering) or even after sampling the signal (post-filtering). In practice, when the signal structure is not entirely known, pre-filtering is used. In this simulation, pre-filtering method is used as well and the Slepian frequency used for generation of various signals in this entire simulation was $c = 2\pi$. The simulation was divided into three main stages where first, results were obtained using an ideal low pass filter for anti-aliasing. Second, results were obtained using a prolate filter for anti-aliasing after which both results were compared to verify if the prolate filter could be used as an anti-aliasing filter.

Consider an input signal as shown in Figure 5.12:

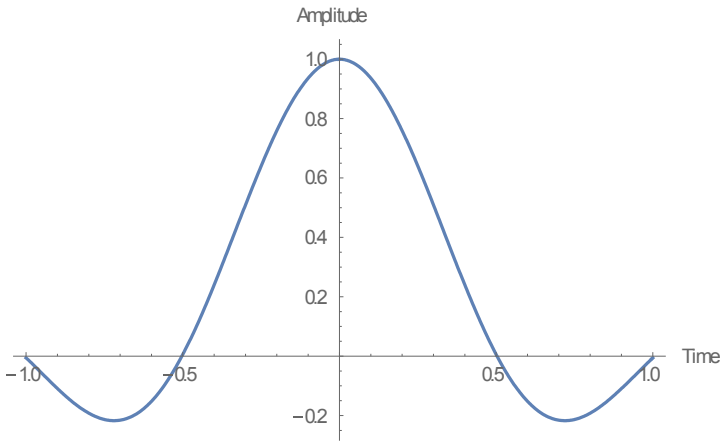

Figure 5.12. Time Domain Response of the Input signal

The frequency response of this signal whose maximum frequency is $f_N = 8.13Hz$ is as seen in Figure 5.13:

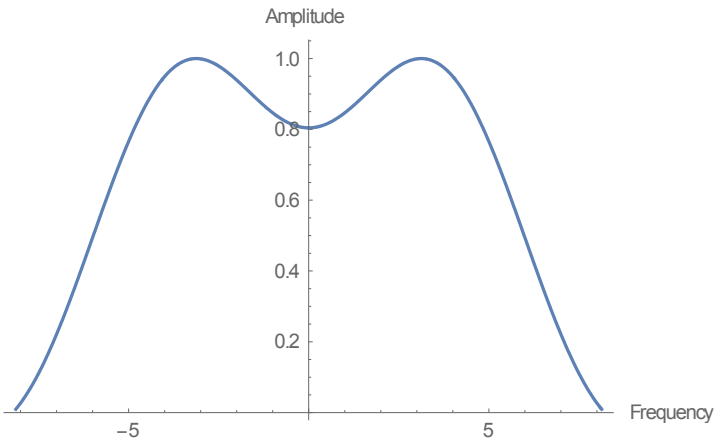

Figure 5.13. Frequency Response of the Input Signal

In order to observe aliasing phenomena in this signal as seen from the previous chapter, the sampling frequency i.e. f_s is kept lower than twice Nyquist frequency i.e. $2f_N$. In the first stage of the simulation, the signal is pre-filtered by an ideal low-pass filter with maximum frequency equal to 8.13Hz which is as seen in Figure 5.14:

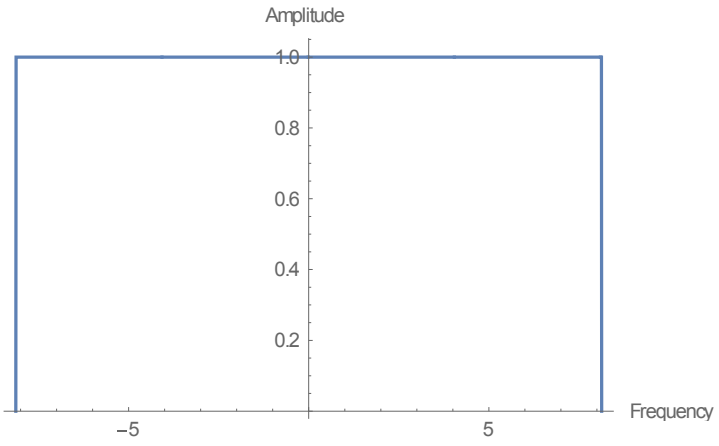

Figure 5.14. Frequency response of ideal low pass anti-aliasing filter

An inverse Fourier transform operation was performed on the resultant pre-filtered output signal in order to obtain the time domain response which is as seen in Figure 5.15:

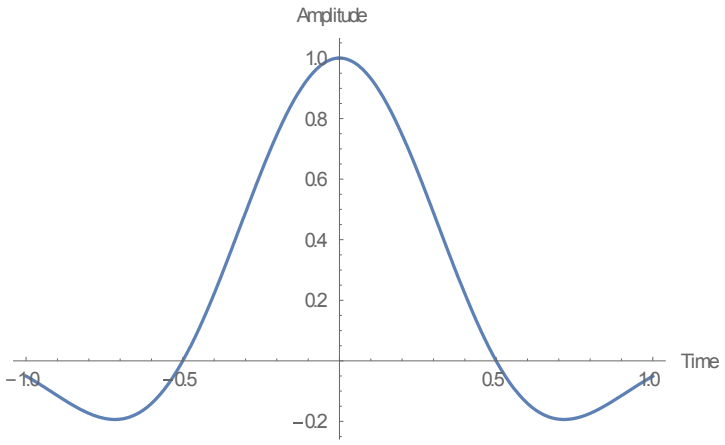

Figure 5.15. Time domain response of the pre-filtered signal

This pre-filtered signal was then sampled with sampling frequency $f_s = 16.2Hz$ which is less than twice the maximum frequency of the input signal $2f_N$, as seen in Figure 5.16:

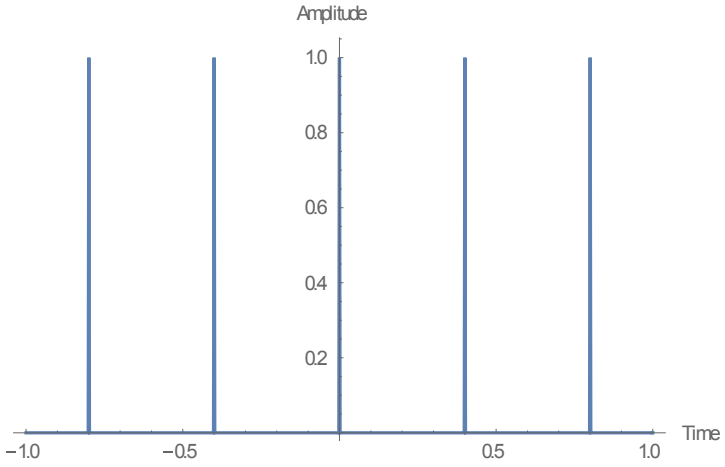

Figure 5.16. Time Domain Response of train of impulses with $f_s = 16.2Hz$

The aliasing was then observed by plotting the frequency response of the sampled signal as seen in Figure 5.17:

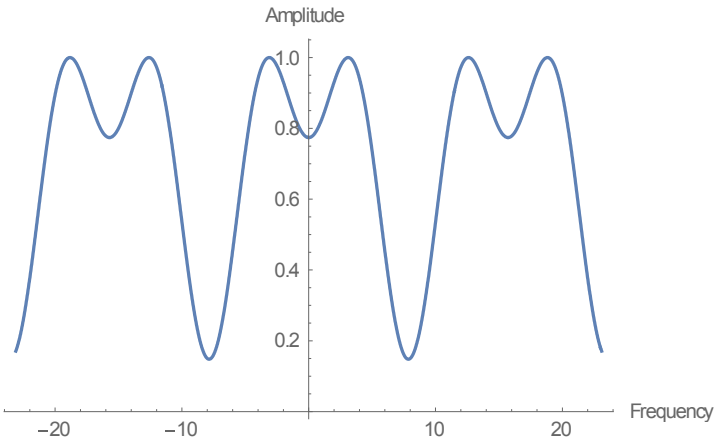

Figure 5.17. Frequency response of the sampled signal using ideal low pass filter

If frequency response of the pre-filtered signal, as seen in Figure 5.17, is compared with the frequency response of the signal without pre-filtering, as seen in Figure 4.14, it is seen that the aliasing present due to lower sampling rate has not reduced. If the bandwidth of the ideal low pass filter is reduced further then the aliasing present in this case can be completely removed but this will cause loss of signal components which is undesirable in baseband applications.

In the next stage of the simulation, a prolate filter was used as a pre-filter with its virtual bandwidth equal to the bandwidth of the ideal low pass filter with maximum frequency equal to 8.13Hz and it physical bandwidth was kept equal to 6.25Hz. A prolate filter with Slepian frequency $c = 2\pi$ was tested but the accuracy of the resultant calculations was not high enough due to which the inverse Fourier transform operation failed. Hence, the Slepian frequency used for the prolate filter in this simulation is $c = 10\pi$. All the steps used for pre-filtering were kept same as the steps in the first stage. The frequency response of the prolate filter and the resultant frequency response of the sampled signal is as seen in Figure 5.18 and Figure 5.19 respectively:

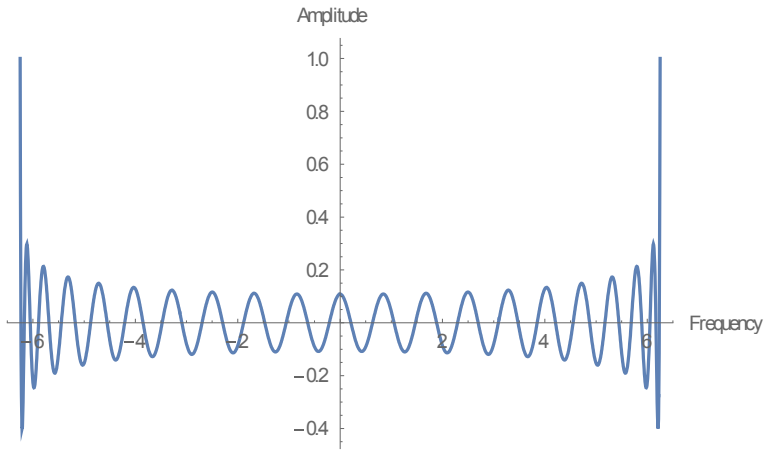

Figure 5.18. Frequency response of the Prolate filter with $c = 10\pi$

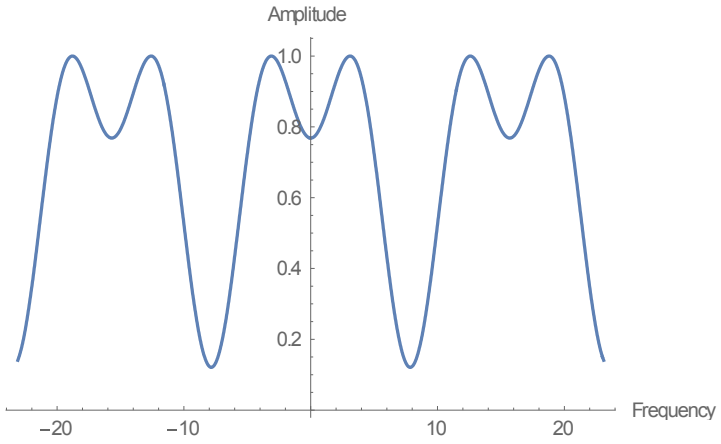

Figure 5.19. Frequency response of sampled signal using prolate filter

If the frequency response of the output sampled signal in Figure 5.19 is observed, it is seen that aliasing is not reduced by using prolate filter for anti-aliasing. Thus, the prolate filter in this instance did not prove to be a good anti-aliasing filter because the virtual bandwidth of the prolate filter was greater than its physical bandwidth. If the virtual bandwidth of the prolate filter is reduced further then it will also reduce the physical bandwidth of the prolate filter which may lead to loss of signal components which is undesirable. But, it is worth noting that even though frequency response of the output sampled signal obtained in both

cases is the same, the bandwidth requirement for the ideal low pass filter case ($BW = 8.13Hz$) is more as compared to the physical bandwidth required by the prolate filter ($BW = 6.25Hz$). The reduced physical bandwidth of the filter will provide various practical advantages such as construction of the filter using cheaper components, reduction in RC losses which will reduce the noise interference in the system.

5.3. Effects of variation of space-bandwidth parameter ‘c’ on the prolate filter

The linear prolate functions used to design prolate filters are dependent on space bandwidth product parameter ‘c’. The prolate filters described until now have a parameter value of $c = 2\pi$. For a total filter bandwidth range of $-10\pi < BW < 10\pi$ and $c = 10\pi$ the reconstruction of an input signal is as seen in Figure 5.20 and Figure 5.21:

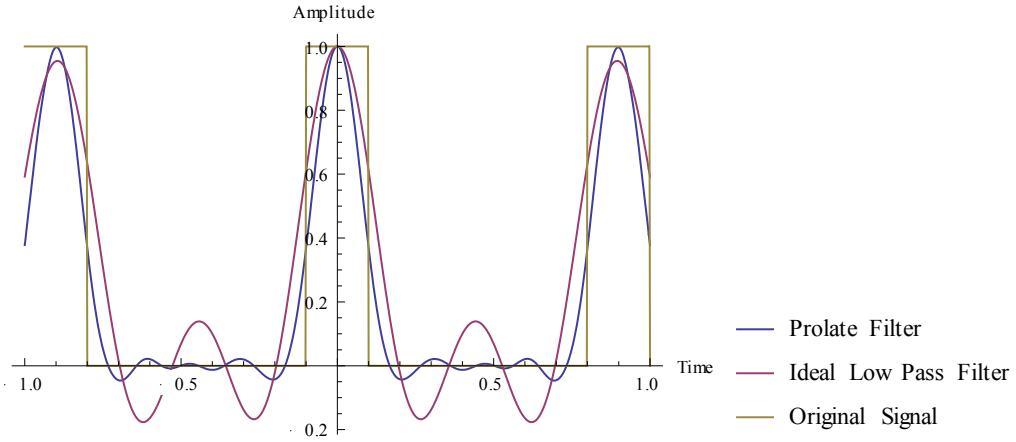

Figure 5.20. Reconstructed Signal obtained from Data Signal – 1001001 with maximum order M = 60 with $c = 10\pi$.

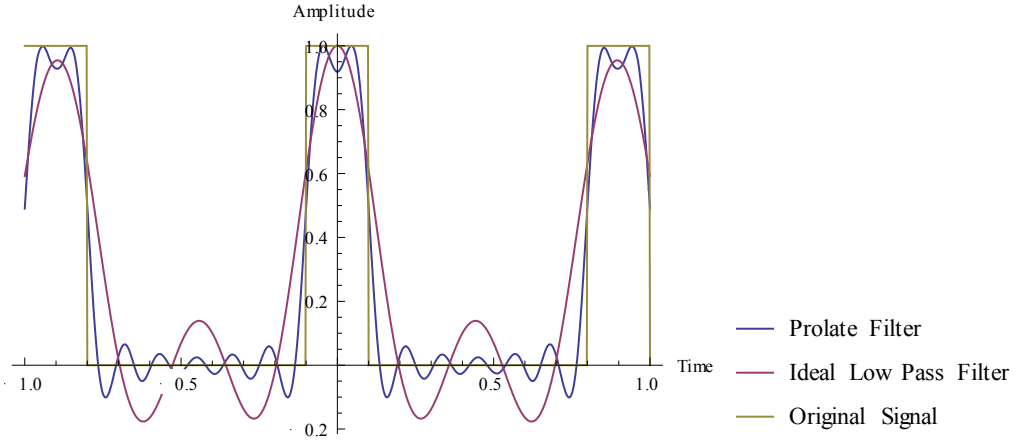

Figure 5.21. Reconstructed Signal obtained from Data Signal – 1001001 with maximum order M = 96 with $c = 10\pi$.

Similarly, for a total filter bandwidth range of $-20\pi < BW < 20\pi$ and $c = 20\pi$ the reconstruction of an input signal is as seen in Figure 5.22 and Figure 5.23:

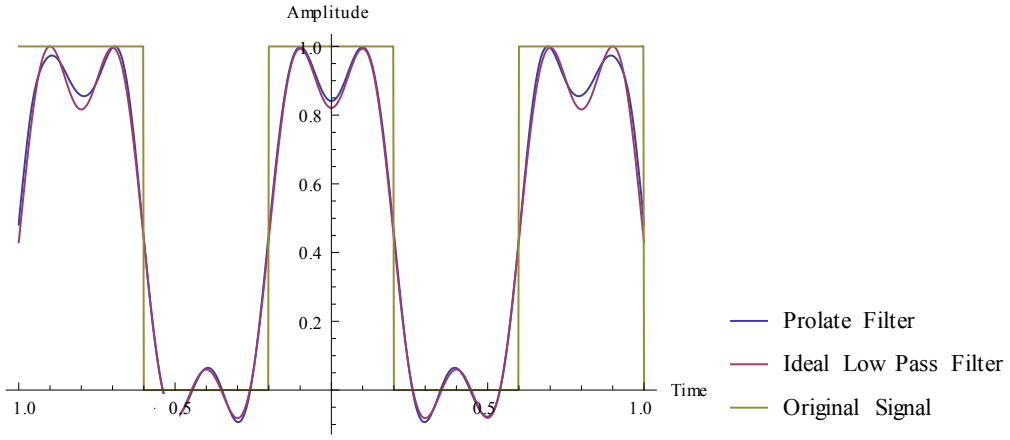

Figure 5.22. Reconstructed Signal obtained from Data Signal – 10101 with maximum order M = 60 with $c = 20\pi$.

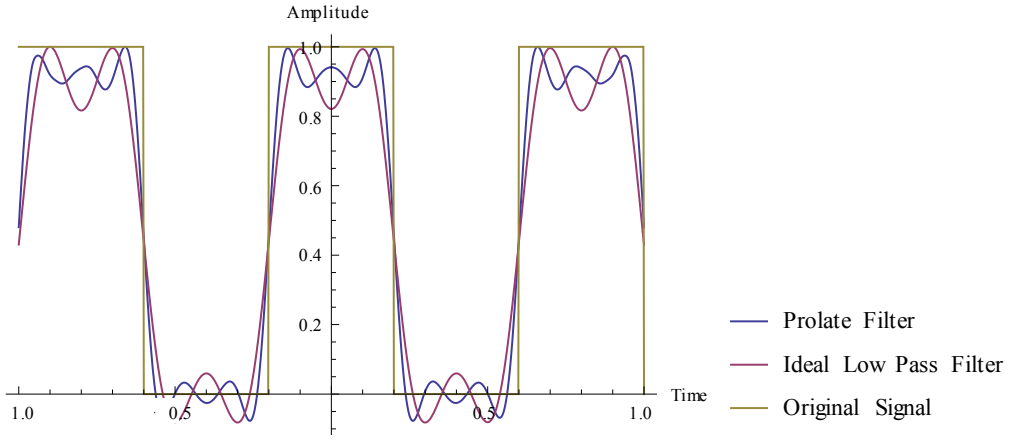

Figure 5.23. Reconstructed Signal obtained from Data Signal – 10101 with maximum order M = 96 with $c = 20\pi$.

For suitable signal reconstruction the value of space-bandwidth parameter 'c' must be equal to or greater than the bandwidth of the channel under consideration as seen in Figure 5.24 for a channel bandwidth of $\pm 2\pi$:

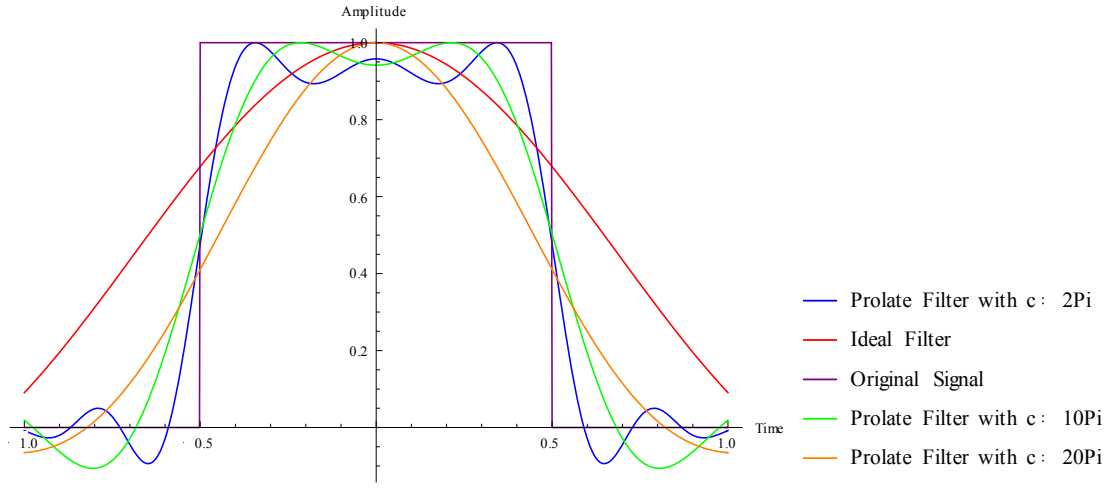

Figure 5.24. Reconstructed Signal using a prolate filter with c ≥ BW of the filter.

If the value of c is less than the bandwidth of the channel, then the prolate filter fails as seen in Figure 5.25 for a channel bandwidth of ±20π:

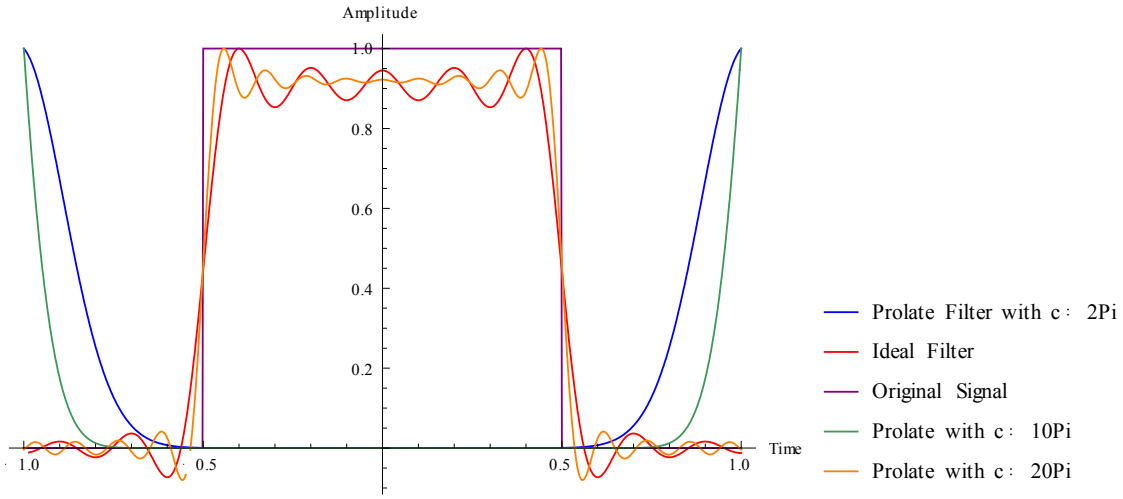

Figure 5.25. Reconstructed Signal using a prolate filter with c ≤ BW of the filter.

5.4. Effects of variation of threshold value 'M' on the prolate filter

The critical value for $c = 2\pi$ is approximately 4 and the threshold value 'M' which provides satisfactory signal reconstruction is equal to 40 or higher which is almost ten times the critical value. Consider a prolate filter with a bandwidth of range $-20\pi < BW < 20\pi$ and $c = 20\pi$. For a threshold value M = 40 the signal reconstruction is as seen in Figure 5.26.

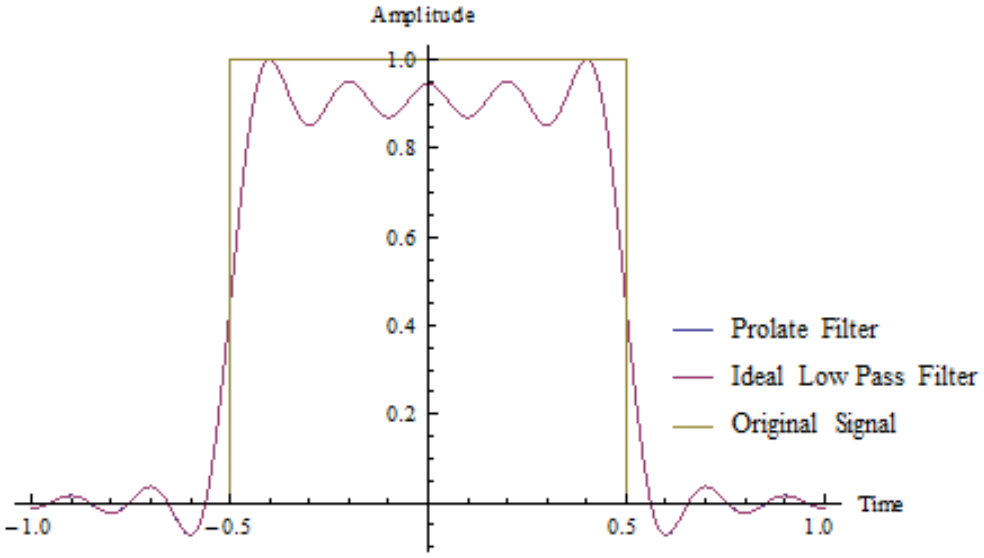

Figure 5.26. Reconstructed Signal for c= 20Pi and M = 40.

The signal reconstruction obtained from a prolate filter is the same as the one obtained from an ideal low pass filter. In order to improve the fit of the signal the extrapolation property is extremely useful. For satisfactory signal reconstruction the threshold value M should be above the critical value $n_{critical}$ as seen in equation (2.24). By using the inherent extrapolation property of the linear prolate functions the orders above $n_{critical}$ can be utilized, thereby using the large amount of energy available outside the interval to improve signal reconstruction as seen in Figure 5.27.

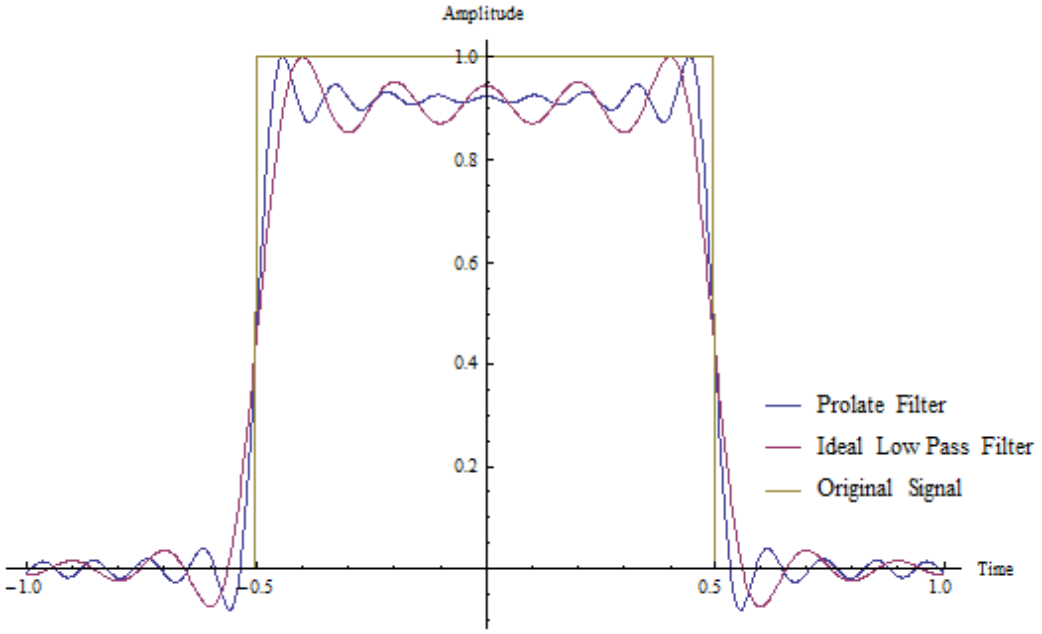

Figure 5.27. Reconstructed Signal for c= 20Pi and M = 96.

Thus, it was shown that a prolate filter can be used to effectively reduce the inter-symbol interference in a baseband communication system. It can also be used as an antialiasing filter in the transmitter section if loss of signal components is acceptable. Additionally, the interference reducing capability of the filter can be improved further by increasing the threshold value 'M' of the prolate filter.

CHAPTER 6: CONCLUSIONS AND FUTURE WORK

6.1. Conclusions

This thesis presents an innovative way to design a filter which can reduce Inter-symbol interference in a baseband communication system. Highly accurate linear prolate functions were used to design the filter. The major advantage of using a prolate filter is that it physically consumes bandwidth similar to an ideal low pass filter while providing an interference reducing capability similar to a low pass filter which has an extended bandwidth. Hence, it can be stated that the prolate filter synthetically increases the bandwidth of the ideal low pass filter. The interference reducing capability of the filter can be further improved by increasing the threshold value 'M' of the filter.

The interference reducing capability of a prolate filter will be same as an ideal low pass filter when the threshold value is equal to $n_{critical}$ given by $\frac{2c}{\pi}$. The artificial increase in bandwidth works only for a threshold value above $n_{critical}$. Furthermore, in order to reduce complexity and to obtain the best interference reduction capability, the value of space-bandwidth parameter 'c' should be equal to the bandwidth required by the channel.

It was also shown that although the filter performance of the prolate filter is similar to that of a normal ideal low pass anti-aliasing filter, its bandwidth requirement is lower as compared to the normal filter. Hence, if the prolate filter is realised physically, its use will lead to use of cheaper components which is practically quite advantageous.

6.2. Future Work

Even though, this research has proved the effectiveness of a prolate filter in reducing Inter-symbol interference in a baseband transmission there is still scope for future work. Firstly, the simulation based results in this thesis can also be obtained in the real world by implementing the prolate filter physically on an integrated circuit (IC). Secondly, in order to further improve the filter performance a comprehensive noise analysis with respect to the linear prolate functions can be done and the complex response of the prolate filter i.e. with respect to phase can also be studied. In Chapter 2: of this thesis, problems in the field of optics and quantum mechanics have been shown to be similar to those in the digital communication or signal processing field. Past literatures [19], [20] have shown that these functions have been used in optics to increase the resolution of a beam by narrowing its point amplitude response. If these highly accurate linear prolate functions can solve the Inter-symbol interference problem in digital communication, they can also be used to solve problems in other fields. Additionally, the increased accuracy of the prolate functions can further improve the results of past literatures. Similarly, the prolate filter can be used in the field of image processing to obtain super resolution in images.

Bibliography

[1] S. Haykin, in *Communication Systems*, John Wiley & Sons Inc., 2008.

[2] B. Lathi, in *Modern Digital and Analog Communication Systems*, Oxford University Press Inc., 1998.

[3] B. Sklar, Digital Communications, Fundamentals and Applications, Prentice Hall , 2001.

[4] H. Nyquist, "Telegraph System for Submarine Cables". Patent 1,922,139, 1932.

[5] D. Slepian, "Some Comments on Fourier Analysis, Uncertainty and Modeling," in *Society for Industrial and Applied Mathematics* , 1983, pp. 379-393.

[6] A. Van Buren, B. King, R. Baier and S. Hanish, in *Tables of Angular Spheroidal Wave Functions, Volume 1; Prolate m = 0*, 1975, pp. 8-15.

[7] D. Slepian and H. Pollack, "Prolate Spheroidal wave functions, Fourier Analysis and uncertainty - I," *Bell Systems Technical Journal,* vol. 40, pp. 43-63, 1961.

[8] B. Frieden, "Evaluation, Design and Extrapolation Methods for Optical Signals, Based on use of the Prolate Functions," *Progress in Optics,* vol. 9, pp. 313-405, 1971.

[9] I. Moore. and M. Cada, "Prolate spheroidal wave functions, an introduction to the Slepian series and its properties," *Applied and Computational Harmonic Analysis,* vol. 16, no. 3, pp. 208-230, 2004.

[10] C. Flammer, Spheroidal Wave Functions, 1957.

[11] I. Moore, *An Introduction to the Slepian series and its applications,* Halifax , 2003.

[12] J. Orlo, "pdfmanual4.com," [Online]. Available: http://pdfmanual4.com/eigenvectors-and-eigenvalues-jeremy-orlo-mit/.

[13] M. Born and E. Wolf, in *Principles of Optics, Electromagnetic Theory of Propagation, Interference and Diffraction of Light*, Pergamon Press, 1959, pp. 413-418.

[14] S. Schelkunoff, "A Mathematical Theory of Linear Arrays," *Bell System Technical Journal,* vol. 22, pp. 80-107, 1943.

[15] G. Francia, "Super Gain Antennas and Optical Resolving Power," *Nuovo Cimento,* vol. 9, no. 3, pp. 426-438, 1952.

[16] H. Osterberg and J. Wilkins, "The resolving Power of a Coated Objective I," *Journal of the Optical Society of America,* vol. 39, pp. 553-557, 1949.

[17] J. Wilkins, "The Resolving Power of a Coated Objective II," *Journal of the Optical Society of America ,* vol. 40, pp. 222-224, 1950.

[18] J. Harris, "Diffraction and Resolving Power," *Journal of Optical Society of America,* vol. 54, pp. 931-936, 1964.

[19] C. Barnes, "Object Restoration in a Diffraction Limited Imaging System," *Journal of Optical Society of America,* vol. 56, pp. 575-578, 1966.

[20] B. Frieden, "On Arbitrarily Perfect Imagery with a Finite Aperture," *Optica Acta: International Journal of Optics,* vol. 16, pp. 795-807, 1969.

[21] A. Devasia and M. Cada, "Bandlimited Signal Extrapolation Using Prolate Spheroidal Wave Functions," *International Journal of Computer Science,* vol. 40, no. 4, pp. 291-300, 2013.

[22] A. Papoulis, "Limits on bandlimited Signals," *Proceedings of the IEEE,* vol. 55, no. 10, pp. 1677 - 1686 , 1967.